AIMS Mathematics, 11(11): 39260–39292.
DOI: 10.3934/math.20261511
Received: 05 September 2026
Revised: 22 October 2026
Accepted: 28 October 2026
Published: 24 November 2026

https://www.aimspress.com/journal/Math

Research article

The Riemann problem and interaction of waves for the Aw–Rascle model with variable velocity offset

Shuzhi Liu* **and Yuanhong Wu**

School of Statistics and Data Science, Ningbo University of Technology, Ningbo, 315211, China

* **Correspondence:** Email: szliu@nbut.edu.cn.

Abstract: This paper investigated the Riemann problem for the Aw–Rascle (AR) traffic flow model with variable velocity offset. The model describes traffic flow under different road conditions, such as the transition from urban roads to rural ones. A stationary wave was introduced in the traffic flow. The resonance phenomena and wave coalescence were analyzed. Uniqueness of the Riemann solution was also discussed. We further studied the interaction of elementary waves case by case, under the framework of the characteristic analysis method. Numerical simulations were presented to validate the analytical results.

Keywords: traffic flow model; variable velocity offset; the Riemann problem; wave interactions
Mathematics Subject Classification: 35L65, 35L80, 35R35

1. Introduction

Traffic flow models are used to describe free-flow states, traffic signal control problems, and traffic jams; they play a pivotal role in urban transportation systems. One of the most popular traffic flow models is the Aw–Rascle (AR) model, which was proposed by Aw and Rascle [1], successfully resolving the theoretical defects of second-order models pointed out by Daganzo [2], and also derived by Zhang [3]. The AR model is formulated as

$$\begin{cases} \rho_t + (\rho u)_x = 0, \\ (\rho(u+p))_t + (\rho u(u+p))_x = 0, \end{cases} \tag{1.1}$$

where $\rho(x,t) \geq 0$ and $u(x,t) \geq 0$ are the density and the velocity of the traffic vehicles on the roadway, respectively. The function $p(\rho)$ is the velocity offset, which is taken as an increasing function of the density. The AR model is appropriate for describing traffic phenomena, such as congestion and stop-and-go waves. It serves as a common tool to explore the generation and evolution of traffic jams [4–6],

and it can also be used to describe the interaction of traffic waves [7–9]. The AR model further lays the foundation for multilane flow formulations, unidirectional road network models, as well as hybrid traffic systems [10–12].

In the original paper [1], the authors considered the prototype of the function $p = \rho^\gamma$. The pressure is a well-defined quantity in fluid flow, but may seem inappropriate for traffic flow. In reality, there is an upper limit to the density of vehicles. In 2008, Berthelin et al. proposed a modified AR model [13], where the velocity offset p takes the form

$$p = \left(\frac{1}{\rho} - \frac{1}{\rho^*}\right)^{-\gamma}, \quad \rho < \rho^*, \tag{1.2}$$

where ρ^* denotes the maximal density of traffic flow and is assumed to be constant. As in the AR model, we assume $\gamma > 0$. The function $p(\rho)$ is defined for $0 < \rho < \rho^*$ and tends to infinity as $\rho \to \rho^*$, which implies that the maximal density cannot be attained. Physically speaking, it means that drivers will tend to avoid absolute jam density. Berthelin et al. further extended the model to a more realistic setting and studied the dynamics of traffic jams [14].

In this paper, we extend the AR model to a more general case by taking road conditions into consideration. It is well-known that drivers react only to what happens in front of them. Existing models, including the AR model and the modified AR model, are built on a unified pressure function, which indicates that the drivers only react to the density of traffic flows ahead. However, when the road conditions change, such as heavy rain or snow, or there is an accident, then drivers should adjust themselves to the new road conditions. This observation motivates us to take different velocity offsets into account. One choice is to consider different γ in (1.2). Other similar choices can be found in [15]. The parameter γ in the equation

$$p = \left(\frac{1}{\rho} - \frac{1}{\rho^*}\right)^{-\gamma}$$

has practical significance in traffic modeling. A larger value of γ indicates greater sensitivity of vehicle speed when the traffic density changes. Since the velocity offset p varies along the road, an additional equation is needed. A trivial equation is given by

$$\gamma_t = 0, \tag{1.3}$$

which means that γ only depends on the spatial variable x. A similar assumption is given in the duct flow [16] or the two-phase flow model [17]. It will be shown that the system belongs to the Temple class in which the characteristics may coincide with each other. However, we prove here that the solution including three waves with zero speeds will not happen, which is apparently different from the Temple class system that we have seen before [18].

In a hyperbolic system, one of the fundamental problems for understanding the system is the Riemann problem. The Riemann solution consists of elementary waves, which can be used to analyze the stability of a system and design numerical methods [19–21], the solution also serves as a foundation for investigating the structure and dynamic behaviours of the system [22–24]. The Riemann problem also plays an important role in dispersive systems [25–27], other practical applications, such as the cavitation of fluid, can be found in [28]. In this paper, we solve the Riemann problem for the AR system (1.1) with (1.3), and the resonance and coalescence of waves are analyzed since the system is not strictly hyperbolic. We should emphasize here that, although the system is similar to duct flows,

the analysis method is different because the parameter γ appears in the elementary waves. Moreover, the sonic speed, which is defined by ρp_ρ, is also a function of γ, which makes it difficult to divide the phase plane into non-overlapping subregions since, across the stationary wave, the curve $u - \rho p_\rho$ changes. To deal with this problem, we analyze the relative positions of the curve $u - \rho p_\rho$ across the stationary wave systematically. Particularly, we deal with the overlapping regions and construct the Riemann solution.

The interaction of elementary waves is an important topic since it can not only help us to investigate the stability of the system, but can also be used to develop related numerical schemes [29, 30]. For the AR traffic flow model, Sun [8] examined the interactions of elementary waves with initial data consisting of three piecewise constant states. Zhang and Sheng [31] investigated wave interactions for the Aw–Rascle model with variable lane widths. Other related works can be found in [32]. We focus on the interaction of waves for the proposed model. Particularly, we study the interaction of shock waves, rarefaction waves, and discontinuity waves with the stationary wave, under the framework of the method of characteristics. When a rarefaction wave (shock wave) interacts with the stationary wave, it will transmit a rarefaction wave (shock wave). When a contact discontinuity interacts with the stationary wave, it will transmit a contact discontinuity and refract a rarefaction wave or a shock wave at the same time.

This paper is organized as follows. In Section 2, we make a detailed method of characteristics for systems (1.1) and (1.3). The elementary waves of the system are introduced, including the rarefaction waves, shock waves, contact discontinuities, and stationary wave. In Section 3, we compare the difference of the original AR model with the modified model. The phase plane is divided into several regions and the overlapping of the splitting curves is discussed. Then, we solve the Riemann problem in the whole phase plane and obtain the solutions by classifying the initial data. We claim that three waves with the same zero speeds cannot occur. The uniqueness of the solution is also discussed. In Section 4, we further explore the interaction of the other elementary waves with the stationary wave. The large-time behavior of the solutions is derived. In Section 5, we present numerical simulations of system (2.1), the results of which are consistent with our analysis.

2. Analysis using the method of characteristics

2.1. Preliminaries

Consider the AR model (1.1) with (1.3):

$$\begin{cases} \rho_t + (\rho u)_x = 0, \\ (\rho(u+p))_t + (\rho u(u+p))_x = 0, \\ \gamma_t = 0, \end{cases} \tag{2.1}$$

where

$$p = \left(\frac{1}{\rho} - \frac{1}{\rho^*}\right)^{-\gamma}.$$

Denote $U = (u, \rho, \gamma)^\top$. Then system (2.1) can be rewritten as

$$A(U)U_t + B(U)U_x = 0,$$

where

$$A(U) = \begin{pmatrix} 0 & 1 & 0 \\ 1 & p_\rho & 0 \\ 0 & 0 & 1 \end{pmatrix}, \qquad B(U) = \begin{pmatrix} \rho & u & 0 \\ u & up_\rho & up_\gamma \\ 0 & 0 & 0 \end{pmatrix}.$$

Here

$$p_\rho = \frac{\gamma}{\rho^2}\left(\frac{1}{\rho} - \frac{1}{\rho^*}\right)^{-\gamma-1}$$

and

$$p_\gamma = -p\ln\left(\frac{1}{\rho} - \frac{1}{\rho^*}\right) = -\left(\frac{1}{\rho} - \frac{1}{\rho^*}\right)^{-\gamma}\ln\left(\frac{1}{\rho} - \frac{1}{\rho^*}\right).$$

The system has three eigenvalues:

$$\lambda_1 = u - \rho p_\rho,\ \lambda_2 = u,\ \lambda_3 = 0.$$

The associated right eigenvectors are

$$\overrightarrow{r_1} = (-p_\rho,\ 1,\ 0)^\top, \quad \overrightarrow{r_2} = (0,\ 1,\ 0)^\top, \quad \overrightarrow{r_3} = (-up_\gamma,\ \rho p_\gamma,\ u - \rho p_\rho)^\top.$$

Since $\nabla\lambda_1 \cdot \overrightarrow{r_1} \neq 0$ and $\nabla\lambda_2 \cdot \overrightarrow{r_2} = \nabla\lambda_3 \cdot \overrightarrow{r_3} = 0$, which indicate that the first characteristic field is genuinely nonlinear, the second and third characteristic fields are linearly degenerate. System (2.1) is non-strictly hyperbolic because λ_1 and λ_2 may coincide with λ_3.

Setting

$$\Gamma_+ : u = \rho p_\rho, \quad \Gamma_- : u = 0,$$

we have

$$\lambda_1 = \lambda_3 \text{ on } \Gamma_+, \quad \lambda_2 = \lambda_3 \text{ on } \Gamma_-.$$

By using the curves Γ_+ and Γ_-, we divide the first quadrant into two regions, namely, D_a and D_b:

$$D_a = \left\{(u,\rho) \mid 0 < u < \rho p_\rho\right\}, \quad D_b = \left\{(u,\rho) \mid u > \rho p_\rho\right\}.$$

Since

$$p_\rho = \frac{\gamma}{\rho^2}\left(\frac{1}{\rho} - \frac{1}{\rho^*}\right)^{-\gamma-1} > 0,$$

it follows that $\rho p_\rho > 0$. Therefore,

$$\lambda_1 = u - \rho p_\rho < 0 = \lambda_3 < \lambda_2 \quad \text{in } D_a$$

and

$$\lambda_3 < \lambda_1 = u - \rho p_\rho < \lambda_2 \quad \text{in } D_b.$$

Consequently, system (2.1) is strictly hyperbolic in both regions.

2.2. The rarefaction waves

We compute the Riemann invariant w_i corresponding to λ_i by solving the following ordinary differential equation:

$$\nabla w_i \cdot \overrightarrow{r_i} = 0, \quad i = 1, 2.$$

For λ_1, the two Riemann invariants are:

$$w_1^1 = u + p, \quad w_1^2 = \gamma.$$

For λ_2, the two Riemann invariants are:

$$w_2^1 = u, \quad w_2^2 = \gamma.$$

Therefore, for a given left-hand state $U_0 = (u_0, \rho_0, \gamma_0)$, the right-hand state $U = (u, \rho, \gamma)$ that can be connected to U_0 by the rarefaction curve is

$$R(U, U_0) : \begin{cases} \xi = \lambda_1 = u - \rho p_\rho, \\ u - u_0 = -p + p_0, \\ \rho < \rho_0, \quad u > u_0. \end{cases} \tag{2.2}$$

Since $p_\rho > 0$, the function $p(\rho)$ is strictly increasing. Therefore, $\rho < \rho_0$ implies $p < p_0$, and hence $u - u_0 = -p + p_0 > 0$. Thus, $\rho < \rho_0$ implies $u > u_0$, see Figure 1.

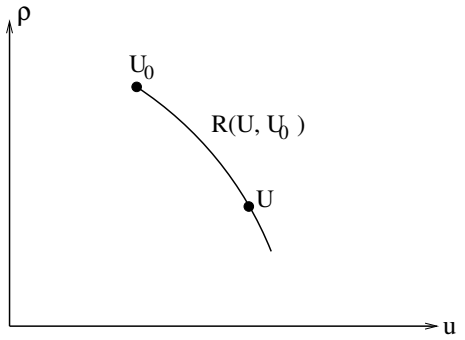


Figure 1. The rarefaction wave for a given U_0.

2.3. The discontinuity solutions

For a discontinuity propagating with the speed $\mathrm{d}x/\mathrm{d}t = \sigma$, the Rankine–Hugoniot condition for system (2.1) is:

$$\begin{cases} \sigma[\rho] = [\rho u], \\ \sigma[\rho(u + p)] = [\rho u(u + p)], \\ \sigma[\gamma] = 0, \end{cases} \tag{2.3}$$

where $[f] := f_1 - f_0$ represents the jump of the function f and σ is the speed of the discontinuity connecting the states U_0 and U_1. Through the last equation of (2.3), either one of the following conditions holds:

(1) $[\gamma] = 0$: U_0 and U_1 are connected by a non-zero speed shock;

(2) $\sigma = 0$: the shock speed vanishes, and we call this a stationary contact discontinuity.

We discuss them separately.

2.3.1. The shock wave and contact discontinuity

For case (1), as the coefficient γ stays invariant, system (2.1) is the same as the original AR model. From (2.3), given the left-hand state $U_0 = (u_0, \rho_0, \gamma_0)$, the right-hand state $U = (u, \rho, \gamma)$, which can be connected to U_0 by the shock curve $S(U, U_0)$, should satisfy

$$S(U, U_0) : \begin{cases} \sigma = \dfrac{\rho u - \rho_0 u_0}{\rho - \rho_0}, \\ u - u_0 = -p + p_0, \\ \rho > \rho_0, \quad u < u_0. \end{cases} \tag{2.4}$$

Moreover, from the second equation of (2.4), we have

$$u = -p + p_0 + u_0.$$

By differentiating it, we get

$$\frac{\mathrm{d}u}{\mathrm{d}\rho} = -\frac{\gamma}{\rho^2}\left(\frac{1}{\rho} - \frac{1}{\rho^*}\right)^{-\gamma-1} < 0,$$

$$\frac{\mathrm{d}^2u}{\mathrm{d}\rho^2} = \frac{\gamma\left(1 - \gamma - \frac{2\rho}{\rho^*}\right)}{\rho^4}\left(\frac{1}{\rho} - \frac{1}{\rho^*}\right)^{-\gamma-2} < 0.$$

Therefore, both the rarefaction and shock wave curves are decreasing in the (u, ρ) plane. The concavity property of the curves may change since the sign of

$$\frac{\mathrm{d}^2u}{\mathrm{d}\rho^2}$$

is not determined. If we further assume that $\gamma > 1$, then

$$\frac{\mathrm{d}^2u}{\mathrm{d}\rho^2} < 0,$$

and one can obtain that both the wave curves are concave. See Figure 2.

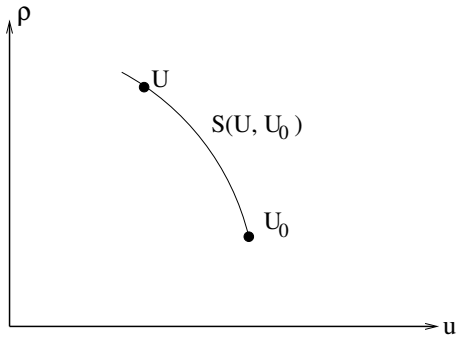


Figure 2. The shock wave for a given U_0.

From (2.3), we also obtain another solution to system (2.1): the contact discontinuity $J(U, U_0)$, which is

$$J(U, U_0) : u = u_0 = \xi, \ \rho \neq \rho_0.$$

2.3.2. The stationary contact discontinuity

For case (2), we search for the time-independent smooth solutions, so that system (2.1) can be written as

$$\begin{cases} (\rho u)' = 0, \\ (\rho u(u+p))' = 0, \end{cases} \tag{2.5}$$

which is equivalent to

$$\begin{cases} \rho u = \rho_0 u_0, \\ u + p = u_0 + p_0. \end{cases} \tag{2.6}$$

Combining the above two equations, we denote

$$F(\rho) := \frac{\rho_0 u_0}{\rho} + p(\rho) - u_0 - p(\rho_0), \tag{2.7}$$

where

$$p(\rho) = \left(\frac{1}{\rho} - \frac{1}{\rho^*}\right)^{-\gamma}.$$

It can be verified that

$$\lim_{\rho \to 0} F(\rho) = +\infty, \quad \lim_{\rho \to \rho^*} F(\rho) = +\infty. \tag{2.8}$$

We compute the derivative of F with respect to ρ and have

$$\frac{\mathrm{d}F(\rho)}{\mathrm{d}\rho} = -\frac{\rho_0 u_0}{\rho^2} + \frac{\gamma}{\rho^2}\left(\frac{1}{\rho} - \frac{1}{\rho^*}\right)^{-\gamma-1}. \tag{2.9}$$

Let

$$\frac{dF(\rho)}{d\rho} = 0,$$

and we obtain the unique root, which is given by

$$\rho_{\min} = \frac{\rho^* (\rho_0 u_0)^{\frac{1}{\gamma+1}}}{\rho^* \gamma^{\frac{1}{\gamma+1}} + (\rho_0 u_0)^{\frac{1}{\gamma+1}}}.$$

Therefore, $F(\rho) = 0$ admits a solution if and only if $F(\rho_{min}) \leq 0$. If $F(\rho_{min}) > 0$, then there is no solution, which indicates that there is no stationary wave. If $F(\rho_{min}) = 0$, there is a unique solution; this case is a degenerate case for $F(\rho_{min}) < 0$ as the two roots coincide. Here and after, we assume $F(\rho_{min}) < 0$ such that there is a stationary contact discontinuity. Combining with (2.8) and (2.9), we have two solutions, which are $\rho_\# < \rho_{min} < \rho^\#$, such that

$$F(\rho_\#) = F(\rho^\#) = 0.$$

Thus, there are two solutions $U_\# = (u_\#, \rho_\#, \gamma)$, $U^\# = (u^\#, \rho^\#, \gamma)$.

Lemma 1. *Given the left-hand state* (u_0, ρ_0, γ_0)*, the states* $U_\# = (u_\#, \rho_\#, \gamma)$ *and* $U^\# = (u^\#, \rho^\#, \gamma)$ *that can be connected with* $S_0(U, U_0)$ *satisfy* $U^\# \in D_a,\ U_\# \in D_b$.

Proof. By the previous analysis, $F(\rho) = 0$ has exactly two roots satisfying $\rho_\# < \rho_{\min} < \rho^\#$, hence

$$\rho_\# < \frac{\rho^* \left(\frac{\rho_0 u_0}{\gamma}\right)^{\frac{1}{\gamma+1}}}{\rho^* + \left(\frac{\rho_0 u_0}{\gamma}\right)^{\frac{1}{\gamma+1}}}.$$

From this, we derive that

$$\frac{\gamma}{\rho_\#}\left(\frac{1}{\rho_\#} - \frac{1}{\rho^*}\right)^{-\gamma-1} < \frac{u_0\rho_0}{\rho_\#} = u_\#,$$

which gives us $U_\# \in D_b$. The proof of $U^\# \in D_a$ is similar, so we omit it. □

From Eq (2.5), we have

$$\begin{cases} u\mathrm{d}\rho + \rho\mathrm{d}u = 0, \\ \mathrm{d}u + \dfrac{\partial p}{\partial \rho}\mathrm{d}\rho + \dfrac{\partial p}{\partial \gamma}\mathrm{d}\gamma = 0. \end{cases} \tag{2.10}$$

By solving (2.10), we obtain

$$\begin{cases} \dfrac{\mathrm{d}u}{\mathrm{d}\gamma} = \dfrac{u\left(\frac{1}{\rho} - \frac{1}{\rho^*}\right)^{-\gamma} \ln\left(\frac{1}{\rho} - \frac{1}{\rho^*}\right)}{u - \frac{\gamma}{\rho}\left(\frac{1}{\rho} - \frac{1}{\rho^*}\right)^{-\gamma-1}}, \\ \dfrac{\mathrm{d}\rho}{\mathrm{d}\gamma} = -\dfrac{\rho\left(\frac{1}{\rho} - \frac{1}{\rho^*}\right)^{-\gamma} \ln\left(\frac{1}{\rho} - \frac{1}{\rho^*}\right)}{u - \frac{\gamma}{\rho}\left(\frac{1}{\rho} - \frac{1}{\rho^*}\right)^{-\gamma-1}}. \end{cases} \tag{2.11}$$

Therefore, the monotone property of curve S_0 depends on the sign of

$$\ln\left(\frac{1}{\rho} - \frac{1}{\rho^*}\right).$$

Without loss of generality, we assume that

$$\ln\left(\frac{1}{\rho} - \frac{1}{\rho^*}\right) > 0$$

in this paper, i.e.,

$$\rho < \frac{\rho^*}{\rho^* + 1}.$$

The other case,

$$\frac{\rho^*}{\rho^* + 1} < \rho < \rho^*,$$

can be discussed similarly. Thus, when

$$u < \frac{\gamma}{\rho}\left(\frac{1}{\rho} - \frac{1}{\rho^*}\right)^{-\gamma-1},$$

we have

$$\frac{\mathrm{d}\rho}{\mathrm{d}\gamma} > 0.$$

As we assume that $\mathrm{d}\gamma > 0$, we have $\mathrm{d}\rho > 0$. On the contrary, when

$$u > \frac{\gamma}{\rho}\left(\frac{1}{\rho} - \frac{1}{\rho^*}\right)^{-\gamma-1},$$

we have $\mathrm{d}\rho < 0$ as $\mathrm{d}\gamma > 0$. The curve of S_0 with respect to γ can be seen in Figure 3.

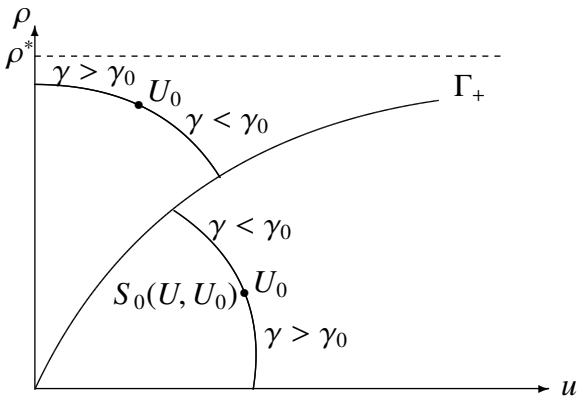


Figure 3. The curve of S_0.

Next, we want to know when the shock speed coincides with the stationary wave. From Eq (2.4), we have

$$\begin{aligned}\sigma &= \frac{\rho u - \rho_0 u_0}{\rho - \rho_0} \\ &= \frac{\rho(u_0 + p_0 - p) - \rho_0 u_0}{\rho - \rho_0} \\ &= u_0 - \frac{\rho(p - p_0)}{\rho - \rho_0}, \quad \rho > \rho_0.\end{aligned}$$

When the shock speed vanishes, setting $\sigma = 0$ gives

$$u_0 = \frac{\rho(p - p_0)}{\rho - \rho_0}, \qquad \rho > \rho_0.$$

By the mean value theorem, there exists $\xi \in (\rho_0, \rho)$ such that

$$\frac{p - p_0}{\rho - \rho_0} = p_\rho(\xi).$$

Hence $u_0 = \rho p_\rho(\xi)$. Since ρp_ρ is strictly increasing with respect to ρ, we obtain

$$u_0 = \frac{\rho(p - p_0)}{\rho - \rho_0} = \rho p_\rho(\xi) > \rho_0 p_\rho(\rho_0) = \frac{\gamma}{\rho_0}\left(\frac{1}{\rho_0} - \frac{1}{\rho^*}\right)^{-\gamma-1}.$$

Therefore, we have $U_0 \in D_b$ and the following lemma.

Lemma 2. *The shock speed $\sigma(U, U_0)$ may change sign along the shock curve $S(U, U_0)$:*
(1) if $U_0 \in D_a$, then $\sigma(U, U_0) < 0$;
(2) if $U_0 \in D_b$, then there exists a point $U = \widetilde{U}_0 \in D_a$ that is on the shock curve $S(U, U_0)$ such that

$$\begin{cases} \sigma(\widetilde{U}_0, U_0) = 0, \\ \sigma(U, U_0) > 0, \ \rho \in (\rho_0, \widetilde{\rho_0}), \\ \sigma(U, U_0) < 0, \ \rho \in (\widetilde{\rho_0}, +\infty). \end{cases}$$

3. The Riemann problem

Consider the Riemann problem of (2.1) equipped with the following data:

$$(u, \rho, \gamma) = \begin{cases} (u_-, \rho_-, \gamma_0), & x < 0, \\ (u_+, \rho_+, \gamma_1), & x > 0, \end{cases} \tag{3.1}$$

where $u_\pm$, $\rho_\pm$, $\gamma_{0,1}$ are constants, and we assume $\gamma_1 > \gamma_0$. To solve the Riemann problem, we know that the coefficients γ_0 and γ_1 are different across the stationary wave, which is the essential difference compared with the original AR model. Thus, in the following sections, we first define two critical curves Γ_0 and Γ_1. In addition, we will show the relations of the shock vanishing points on both sides of the stationary wave (Lemma 3). The uniqueness of the solution also needs to be classified (Lemma 4). The resonance phenomenon as the rarefaction wave attached to the stationary wave is also examined (Lemma 6).

3.1. The positions of Γ_0 and Γ_1

Throughout this subsection, we assume $\gamma_1 > \gamma_0$, as stated in the Riemann initial data (3.1). Consider the following curves:

$$\Gamma_0 : \ u = \frac{\gamma_0}{\rho}\left(\frac{1}{\rho} - \frac{1}{\rho^*}\right)^{-\gamma_0 - 1}, \quad \Gamma_1 : \ u = \frac{\gamma_1}{\rho}\left(\frac{1}{\rho} - \frac{1}{\rho^*}\right)^{-\gamma_1 - 1},$$

which are the critical curves corresponding to the coefficients γ_0 and γ_1, respectively. When the two curves intersect, we have

$$\frac{\gamma_0}{\rho}\left(\frac{1}{\rho} - \frac{1}{\rho^*}\right)^{-\gamma_0 - 1} = \frac{\gamma_1}{\rho}\left(\frac{1}{\rho} - \frac{1}{\rho^*}\right)^{-\gamma_1 - 1}.$$

We can solve for ρ and obtain

$$\rho = \frac{1}{\left(\frac{\gamma_1}{\gamma_0}\right)^{\frac{1}{\gamma_1 - \gamma_0}} + \frac{1}{\rho^*}},$$

which yields that $\rho < \rho^*$. Denote the intersection point of Γ_0 and Γ_1 as $U_s = (u_s, \rho_s)$, and therefore, the (u, ρ) plane can be divided into four distinct regions, which are determined by the intersection and relative positioning of the curves Γ_0, denoted as D_1, D_2, D_3, D_4, as illustrated in Figure 4.

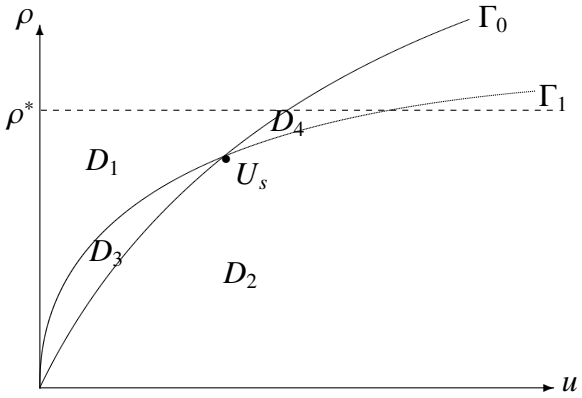


Figure 4. The positions of Γ_0, Γ_1, and the four regions.

3.2. The positions of $\widetilde{U}_-$ and $\widetilde{U}_{-\#}$

Lemma 3. *Assume that $U_- \in D_2$ and $U_{-\#} \in S_0(U, U_-)$. From Lemma 2, there exist $\widetilde{U}_- \in S(U, U_-)$ and $\widetilde{U}_{-\#} \in S(U, U_{-\#})$, at which both the shocks have zero speed. For convenience, we introduce the one-parameter family of curves*

$$u = c\frac{\gamma}{\rho}\left(\frac{1}{\rho} - \frac{1}{\rho^*}\right)^{-\gamma-1}, c > 0,$$

which reduces to the critical curve Γ when $c = 1$. Denote the curves

$$\widetilde{\Gamma}_- : \widetilde{u}_- = c_1\frac{\gamma_0}{\widetilde{\rho}_-}\left(\frac{1}{\widetilde{\rho}_-} - \frac{1}{\rho^*}\right)^{-\gamma_0-1}$$

and

$$\widetilde{\Gamma}_{-\#} : \widetilde{u}_{-\#} = c_2\frac{\gamma_1}{\widetilde{\rho}_{-\#}}\left(\frac{1}{\widetilde{\rho}_{-\#}} - \frac{1}{\rho^*}\right)^{-\gamma_1-1}.$$

We can conclude that $c_1 > c_2$, i.e., $\widetilde{U}_-$ is closer to Γ_+ than $\widetilde{U}_{-\#}$, see Figure 5.

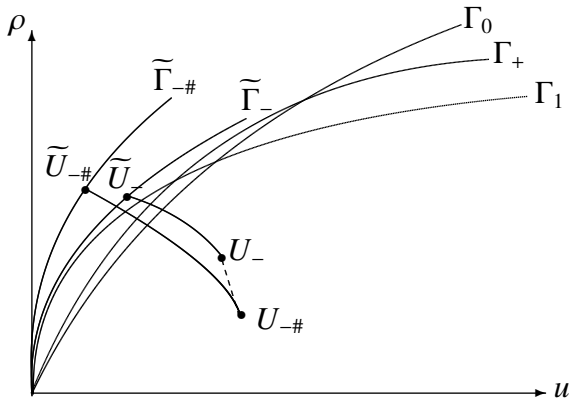


Figure 5. The positions of $\widetilde{U}_-$ and $\widetilde{U}_{-\#}$.

Proof. From the assumption, we have

$$\begin{cases} \rho_- u_- = \widetilde{\rho}_- \widetilde{u}_-, \\ u_- + p_- = \widetilde{u}_- + \widetilde{p}_-. \end{cases} \tag{3.2}$$

From the first equation, we have

$$\widetilde{u}_- = \frac{\rho_- u_-}{\widetilde{\rho}_-}.$$

Let us denote

$$u_- = c_0 \frac{\gamma_0}{\rho_-} \left(\frac{1}{\rho_-} - \frac{1}{\rho^*} \right)^{-\gamma_0 - 1}.$$

Then it follows that

$$(c_0\gamma_0 + 1) \left(\frac{\frac{1}{\rho_-} - \frac{1}{\rho^*}}{\frac{1}{\widetilde{\rho}_-} - \frac{1}{\rho^*}} \right)^{-\gamma_0} = c_0\gamma_0 \left(\frac{\frac{1}{\rho_-} - \frac{1}{\rho^*}}{\frac{1}{\widetilde{\rho}_-} - \frac{1}{\rho^*}} \right)^{-\gamma_0 - 1} + 1.$$

Let

$$x = \left(\frac{\frac{1}{\rho_-} - \frac{1}{\rho^*}}{\frac{1}{\widetilde{\rho}_-} - \frac{1}{\rho^*}} \right)^{-1}.$$

Then

$$F(x) = c_0\gamma_0 x^{\gamma_0 + 1} - (c_0\gamma_0 + 1)x^{\gamma_0} + 1 = 0.$$

This equation has two solutions: $x_1 = 1$ and $x_2 < 1$.

Therefore, we have

$$\frac{1}{\rho_-} - \frac{1}{\rho^*} = \frac{1}{x_2} \left(\frac{1}{\widetilde{\rho}_-} - \frac{1}{\rho^*} \right),$$

leading to

$$\widetilde{u}_- = c_0\gamma_0 \frac{1}{\widetilde{\rho}_-} \left(\frac{1}{\rho_-} - \frac{1}{\rho^*} \right)^{-\gamma_0 - 1} = c_0 x_2^{\gamma_0 + 1} \frac{\gamma_0}{\widetilde{\rho}_-} \left(\frac{1}{\widetilde{\rho}_-} - \frac{1}{\rho^*} \right)^{-\gamma_0 - 1}.$$

This implies $c_1 = c_0 x_2^{\gamma_0 + 1}$. Substituting

$$x_2 = \left(\frac{c_1}{c_0} \right)^{\frac{1}{\gamma_0 + 1}}$$

into $F(x)$, we get

$$(c_0\gamma_0 + 1)c^{-\frac{\gamma_0}{\gamma_0 + 1}} = (c_1\gamma_0 + 1)c_1^{-\frac{\gamma_0}{\gamma_0 + 1}}.$$

Differentiating the above formulae on both sides, we obtain

$$\frac{\left(1 - \frac{1}{c_0}\right)\gamma_0}{\gamma_0 + 1} c_0^{-\frac{\gamma_0}{\gamma_0 + 1}} dc_0 = \frac{\left(1 - \frac{1}{c_1}\right)\gamma_0}{\gamma_0 + 1} c_1^{-\frac{\gamma_0}{\gamma_0 + 1}} dc_1.$$

Since $c_0 > 1$ and $c_1 < 1$, we have $dc_0 \cdot dc_1 < 0$.

Since

$$\frac{u_-}{\frac{\gamma_0}{\rho_-} \left(\frac{1}{\rho_-} - \frac{1}{\rho^*} \right)^{-\gamma_0 - 1}} < \frac{u_{-\#}}{\frac{\gamma_1}{\rho_{-\#}} \left(\frac{1}{\rho_{-\#}} - \frac{1}{\rho^*} \right)^{-\gamma_1 - 1}},$$

we conclude that

$$\frac{\widetilde{u}_-}{\frac{\gamma_0}{\widetilde{\rho}_-}\left(\frac{1}{\widetilde{\rho}_-}-\frac{1}{\rho^*}\right)^{-\gamma_0-1}} > \frac{\widetilde{u}_{-\#}}{\frac{\gamma_1}{\widetilde{\rho}_{-\#}}\left(\frac{1}{\widetilde{\rho}_{-\#}}-\frac{1}{\rho^*}\right)^{-\gamma_1-1}}.$$

Hence, $c_1 > c_2$. □

3.3. The positions of $\widetilde{U}_-^{\#}$ and $\widetilde{U}_{-\#}$

Lemma 4. *Suppose $U_- \in D_2$. There exist two states $\widetilde{U}_- \in S(U, U_-)$ and $\widetilde{U}_{-\#} \in S(U, U_{-\#})$, where both the shock speeds vanish. Additionally, let $U_{-\#} \in S_0(U, U_-)$ and $\widetilde{U}_-^{\#} \in S_0(U, \widetilde{U}_-)$, with the parameter γ jumping from the left state γ_0 to the right state γ_1. Since $\gamma_1 > \gamma_0$, the stationary-wave curve has a unique admissible branch. It follows that $\widetilde{U}_-^{\#}$ coincides with $\widetilde{U}_{-\#}$, as shown in Figure 6.*

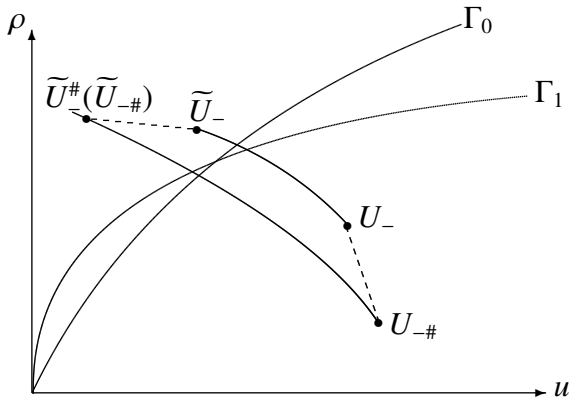


Figure 6. The positions of $\widetilde{U}_-^{\#}$ and $\widetilde{U}_{-\#}$.

Proof. From the assumption, we have the following relations for the states $\widetilde{U}_{-\#}$ and $\widetilde{U}_-^{\#}$:

$$\begin{cases} \widetilde{\rho}_{-\#}\widetilde{u}_{-\#} = \rho_{-\#}u_{-\#} = \rho_- u_-, \\ \widetilde{u}_{-\#} + \left(\frac{1}{\widetilde{\rho}_{-\#}} - \frac{1}{\rho^*}\right)^{-\gamma_1} = u_{-\#} + \left(\frac{1}{\rho_{-\#}} - \frac{1}{\rho^*}\right)^{-\gamma_1} = u_- + \left(\frac{1}{\rho_-} - \frac{1}{\rho^*}\right)^{-\gamma_0}, \end{cases}$$

$$\begin{cases} \widetilde{\rho}_-^{\#}\widetilde{u}_-^{\#} = \widetilde{\rho}_-\widetilde{u}_- = \rho_- u_-, \\ \widetilde{u}_-^{\#} + \left(\frac{1}{\widetilde{\rho}_-^{\#}} - \frac{1}{\rho^*}\right)^{-\gamma_1} = \widetilde{u}_- + \left(\frac{1}{\widetilde{\rho}_-} - \frac{1}{\rho^*}\right)^{-\gamma_0} = u_- + \left(\frac{1}{\rho_-} - \frac{1}{\rho^*}\right)^{-\gamma_0}. \end{cases}$$

By combining these equations, we obtain

$$\begin{cases} \widetilde{\rho}_{-\#}\widetilde{u}_{-\#} = \widetilde{\rho}_-^{\#}\widetilde{u}_-^{\#} = \rho_- u_-, \\ \widetilde{u}_{-\#} + \left(\frac{1}{\widetilde{\rho}_{-\#}} - \frac{1}{\rho^*}\right)^{-\gamma_1} = \widetilde{u}_-^{\#} + \left(\frac{1}{\widetilde{\rho}_-^{\#}} - \frac{1}{\rho^*}\right)^{-\gamma_1} = u_- + \left(\frac{1}{\rho_-} - \frac{1}{\rho^*}\right)^{-\gamma_0}. \end{cases}$$

Therefore, $(\widetilde{u}_{-\#}, \widetilde{\rho}_{-\#})$ and $(\widetilde{u}_-^{\#}, \widetilde{\rho}_-^{\#})$ are both the solutions to the following equations:

$$\begin{cases} \rho u = \rho_- u_-, \\ u + \left(\frac{1}{\rho} - \frac{1}{\rho^*}\right)^{-\gamma_1} = u_- + \left(\frac{1}{\rho_-} - \frac{1}{\rho^*}\right)^{-\gamma_0}. \end{cases}$$

By Lemma 1, this system has two solutions: $U^{\#} \in D_a$ and $U_{\#} \in D_b$. Since both $\widetilde{U}_{-\#}$ and $\widetilde{U}_{-}^{\#}$ lie in D_a, it follows that $\widetilde{U}_{-}^{\#}$ coincides with $\widetilde{U}_{-\#}$. □

Remark 5. Lemma 4 indicates that, when $\widetilde{U}_{-}^{\#}$ and $\widetilde{U}_{-\#}$ coincide, the following two solution structures admit smooth transitions: One is the solution that begins with a stationary wave, followed by a standing shock wave, while the other one begins with a standing shock wave, followed by a stationary wave. Moreover, since the stationary-wave curve and the standing-shock curve intersect at most at one state, any additional zero-speed wave beyond the two-wave configuration must be trivial. Therefore, three nontrivial coinciding zero-speed waves cannot occur in the present model. This differs from certain Temple class systems, where wave curves may overlap along a nontrivial segment and allow multiple intermediate states connected by waves to have the same characteristic speed [33].

3.4. The positions of $U_{c\#}$ and Γ_1

Lemma 6. *Let $U_- \in D_1$. There exists $U_c = (u_c, \rho_c, \gamma_0)$ such that $\{U_c\} = R(U, U_-) \cap \Gamma_0$, with $u_c > u_s$. U_c jumps to $U_{c\#} = (u_{c\#}, \rho_{c\#}, \gamma_1)$ by a stationary wave $S_0(U, U_c)$. Furthermore, the relative position of $U_{c\#}$ and Γ_1 is determined by the following conditions (Figure 7):*
(1) $U_{c\#} \in D_2$, if

$$\rho_{c\#} < \frac{\gamma_0(\gamma_1+1)\rho_c\rho^*}{\gamma_0(\gamma_1+1)\rho_c + \gamma_1(\gamma_0+1)(\rho^*-\rho_c)},$$

(2) $U_{c\#} \in D_4$, if

$$\rho_{c\#} > \frac{\gamma_0(\gamma_1+1)\rho_c\rho^*}{\gamma_0(\gamma_1+1)\rho_c + \gamma_1(\gamma_0+1)(\rho^*-\rho_c)}.$$

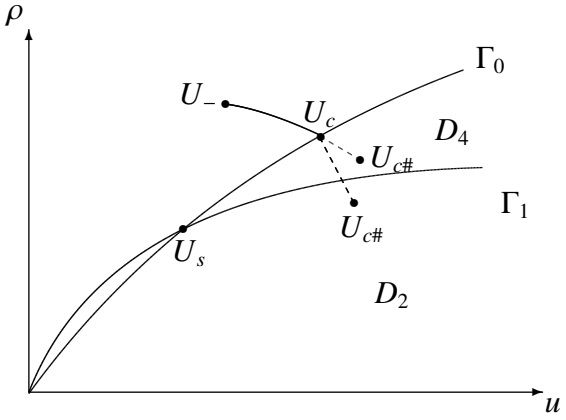


Figure 7. The positions of $U_{c\#}$ and Γ_1.

Proof. Since $U_c = (u_c, \rho_c, \gamma_0) \in \Gamma_0$, we have

$$u_c = \frac{\gamma_0}{\rho_c}\left(\frac{1}{\rho_c} - \frac{1}{\rho^*}\right)^{-\gamma_0-1}. \tag{3.3}$$

Furthermore, considering the stationary wave $S_0(U_{c\#}, U_c)$, we have

$$\begin{cases} \rho_{c\#}u_{c\#} = \rho_c u_c, \\ u_{c\#} + \left(\dfrac{1}{\rho_{c\#}} - \dfrac{1}{\rho^*}\right)^{-\gamma_1} = u_c + \left(\dfrac{1}{\rho_c} - \dfrac{1}{\rho^*}\right)^{-\gamma_0}. \end{cases} \tag{3.4}$$

By combining Eqs (3.3) and (3.4), we obtain

$$\begin{cases} \rho_{c\#}u_{c\#} = \gamma_0\left(\dfrac{1}{\rho_c}-\dfrac{1}{\rho^*}\right)^{-\gamma_0-1}, \\ u_{c\#}+\left(\dfrac{1}{\rho_{c\#}}-\dfrac{1}{\rho^*}\right)^{-\gamma_1} = \left(\dfrac{\gamma_0+1}{\rho_c}-\dfrac{1}{\rho^*}\right)\left(\dfrac{1}{\rho_c}-\dfrac{1}{\rho^*}\right)^{-\gamma_0-1}. \end{cases} \tag{3.5}$$

Differentiating the above equations with respect to $u_{c\#}$, $\rho_{c\#}$, ρ_c, then eliminating $\mathrm{d}\rho_c$, and substituting $u_{c\#}$ from the second equation in (3.5), we have

$$\frac{\mathrm{d}u_{c\#}}{\mathrm{d}\rho_{c\#}} = \frac{1}{\rho_c-\rho_{c\#}}\left[\frac{(\gamma_0+1)\rho^*-\rho_c}{\rho^*-\rho_c}\left(\frac{1}{\rho_c}-\frac{1}{\rho^*}\right)^{-\gamma_0}-\left(\frac{1}{\rho_{c\#}}-\frac{1}{\rho^*}\right)^{-\gamma_1}\right]. \tag{3.6}$$

From the second equation of (3.4), we have

$$\left(\frac{1}{\rho_c}-\frac{1}{\rho^*}\right)^{-\gamma_0} > \left(\frac{1}{\rho_{c\#}}-\frac{1}{\rho^*}\right)^{-\gamma_1} \quad \text{as} \quad u_{c\#} > u_c.$$

Thus, we conclude that

$$\frac{\mathrm{d}u_{c\#}}{\mathrm{d}\rho_{c\#}} > 0,$$

which means the curve $S_0(U_{c\#}, U_c)$ is increasing.

From the first equation in (3.5), we have

$$\left(\frac{1}{\rho_c}-\frac{1}{\rho^*}\right)^{-\gamma_0-1} = \frac{\rho_{c\#}u_{c\#}}{\gamma_0}.$$

Substituting this into the second equation, and by rearranging the terms, we obtain

$$u_{c\#}\left(\frac{\gamma_0\gamma_1\rho^*(\rho_{c\#}-\rho_c)+\gamma_1\rho_{c\#}(\rho^*-\rho_c)}{\gamma_0\rho_c(\rho^*-\rho_{c\#})}\right) = \frac{\gamma_1}{\rho_{c\#}}\left(\frac{1}{\rho_{c\#}}-\frac{1}{\rho^*}\right)^{-\gamma_1-1}.$$

Since the expression for the curve Γ_1 is given by

$$u = \frac{\gamma_1}{\rho}\left(\frac{1}{\rho}-\frac{1}{\rho^*}\right)^{-\gamma_1-1},$$

and it is increasing, we only need to compare which one of

$$\frac{\gamma_0\gamma_1\rho^*(\rho_{c\#}-\rho_c)+\gamma_1\rho_{c\#}(\rho^*-\rho_c)}{\gamma_0\rho_c(\rho^*-\rho_{c\#})}$$

and 1 is greater. Therefore, defining the function

$$H(\rho_{c\#}) = \frac{\gamma_0\gamma_1\rho^*(\rho_{c\#}-\rho_c)+\gamma_1\rho_{c\#}(\rho^*-\rho_c)}{\gamma_0\rho_c(\rho^*-\rho_{c\#})}-1,$$

we differentiate $H(\rho_{c\#})$ with respect to $\rho_{c\#}$ to obtain

$$\frac{\mathrm{d}H(\rho_{c\#})}{\mathrm{d}\rho_{c\#}} = \frac{\gamma_1\rho^*(\gamma_0+1)(\rho^*-\rho_c)}{\gamma_0\rho_c(\rho^*-\rho_{c\#})^2} > 0.$$

Since

$$\lim_{\rho_{c\#}\to 0} H(\rho_{c\#}) = -\gamma_0 - 1 < 0, \quad \lim_{\rho_{c\#}\to\rho^*} H(\rho_{c\#}) = +\infty, \tag{3.7}$$

we solve $H(\rho_{c\#}) = 0$ and obtain

$$\rho_{c\#} = \frac{\gamma_0(\gamma_1+1)\rho_c\rho^*}{\gamma_0(\gamma_1+1)\rho_c + \gamma_1(\gamma_0+1)(\rho^*-\rho_c)} < \rho^*.$$

Therefore, we have

$$\begin{cases} u_{c\#} > \dfrac{\gamma_1}{\rho_{c\#}}\left(\dfrac{1}{\rho_{c\#}} - \dfrac{1}{\rho^*}\right)^{-\gamma_1-1}, & \text{if} \quad \rho_{c\#} < \dfrac{\gamma_0(\gamma_1+1)\rho_c\rho^*}{\gamma_0(\gamma_1+1)\rho_c + \gamma_1(\gamma_0+1)(\rho^*-\rho_c)}, \\ u_{c\#} < \dfrac{\gamma_1}{\rho_{c\#}}\left(\dfrac{1}{\rho_{c\#}} - \dfrac{1}{\rho^*}\right)^{-\gamma_1-1}, & \text{if} \quad \rho_{c\#} > \dfrac{\gamma_0(\gamma_1+1)\rho_c\rho^*}{\gamma_0(\gamma_1+1)\rho_c + \gamma_1(\gamma_0+1)(\rho^*-\rho_c)}. \end{cases}$$

Eventually, we have proved the lemma. □

In the following part, we only consider the case $U_{c\#} \in D_2$ since the case $U_{c\#} \in D_4$ can be treated similarly without additional difficulties.

3.5. The Riemann solution

In this section, we will construct the Riemann solution case by case based on the previous analysis.
Case 1. $U_- \in D_2$. Define three points $U_{-\#} \in D_2$, $\widetilde{U}_{-\#} \in D_1$, and $\widetilde{U}_- \in D_1$. Here, $U_{-\#} \in S_0(U, U_-)$, $\widetilde{U}_- \in S(U, U_-)$, and $\widetilde{U}_{-\#} \in S(U, U_{-\#})$ such that the shock speed vanishes, in view of Lemma 2. Next, we draw the curve $R(U, U_{-\#})$, which intersects the u-axis at $\bar{U} = (\bar{u}, 0)$, and $\bar{u} = u_{-\#} + p_{-\#}$. This configuration is illustrated in Figure 8.

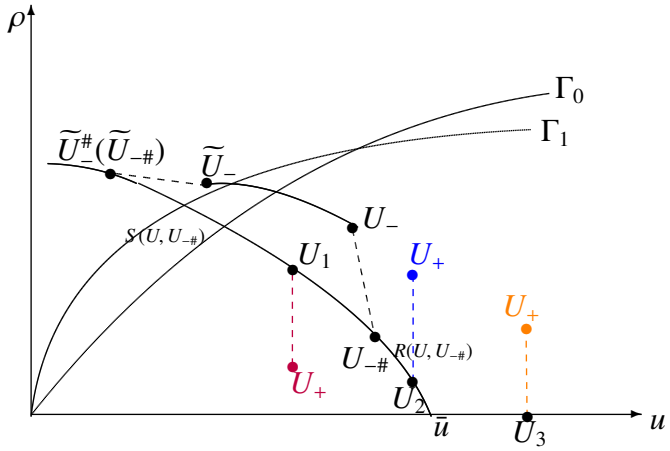


Figure 8. Case 1.1–1.3. $U_- \in D_2$.

Case 1.1. $\widetilde{u}_{-\#} < u_+ < u_{-\#}$. The corresponding state on the shock curve $S(U, U_{-\#})$ lies before the zero-speed point $\widetilde{U}_{-\#}$. Hence, by Lemma 2, the shock speed is positive. Denote $J(U_+, U) \cap S(U, U_{-\#}) = \{U_1\}$. The Riemann solution is (see Figure 9(a)) $S_0(U_{-\#}, U_-) \to S(U_1, U_{-\#}) \to J(U_+, U_1)$.

Case 1.2. $u_{-\#} < u_+ < \bar{u}$. Denote

$$J(U_+, U) \cap R(U, U_{-\#}) = \{U_2\}.$$

The Riemann solution is (see Figure 9(b))

$$S_0(U_{-\#}, U_-) \to R(U_2, U_{-\#}) \to J(U_+, U_2).$$

Case 1.3. $\bar{u} < u_+$. Denote $J(U_+, U) \cap \{\rho = 0\} = \{U_3\}$. The Riemann solution is (see Figure 9(c))

$$S_0(U_{-\#}, U_-) \to R(\bar{U}, U_{-\#}) \to \text{Vacuum} \to J(U_+, U_3).$$

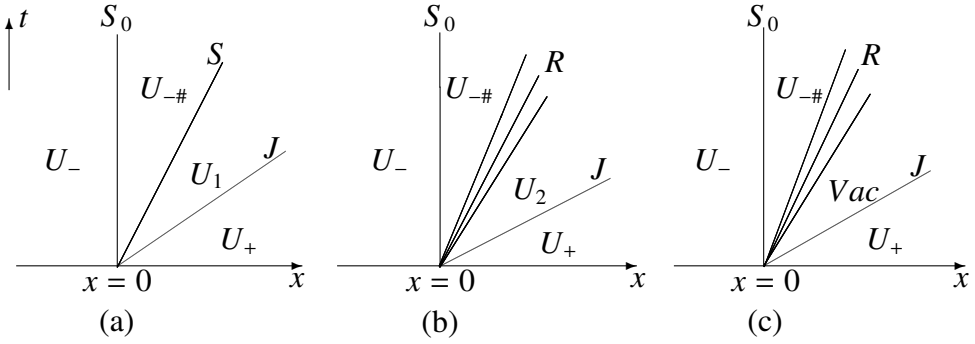


Figure 9. Case 1.1–1.3. (a) $\widetilde{u}_{-\#} < u_+ < u_{-\#}$; (b) $u_{-\#} < u_+ < \bar{u}$; (c) $\bar{u} < u_+$.

Case 1.4. $0 < u_+ < \widetilde{u}_{-\#}$. The shock lies on the negative-speed branch described in Lemma 2. Hence $\sigma(U_1, U_{-\#}) < 0 = \lambda_3 < \lambda_2$, which guarantees the correct ordering of the shock wave, stationary wave, and contact discontinuity. For any point $U \in S(U, \widetilde{U}_-)$ with $\rho > \widetilde{\rho}_-$, it jumps to some state $U^\#$ by a stationary wave and such states form the curve $S_0(U^\#, U)$. Denote $J(U_+, U) \cap S_0(U^\#, U) = \{U_4^\#\}$, $U_4^\#$ is jumped by stationary wave $S_0(U_4^\#, U_4)$, and $U_4 \in S(U, U_-)$, see Figure 10. The Riemann problem in this case is

$$S(U_4, U_-) \to S_0(U_4^\#, U_4) \to J(U_+, U_4^\#).$$

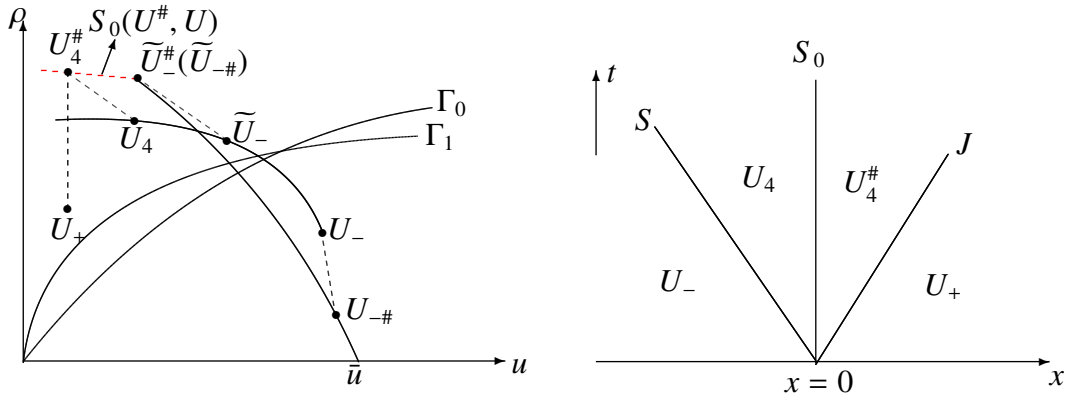


Figure 10. Case 1.4. $0 < u_+ < \widetilde{u}_{-\#}$.

Case 2. $U_- \in D_1$. In this case, both the rarefaction wave and the shock wave have negative speeds. We denote $\{U_c\} = R(U, U_-) \cap \Gamma_0$. A stationary wave jumps from U_c to $U_{c\#} \in D_2$. We draw the curve $R(U, U_{C\#})$, which intersects with the u-axis at $\bar{U} = (\bar{u}, 0)$. From Lemma 2, we have $\widetilde{U}_{c\#} \in S(U, U_{c\#})$ at which the shock speed vanishes. Since Γ_0 and Γ_1 intersect at point $U_s = (u_s, \rho_s)$, we discuss the following two cases, $u_c < u_s$ and $u_c > u_s$.

Case 2.1. $u_c < u_s$, see Figure 11.

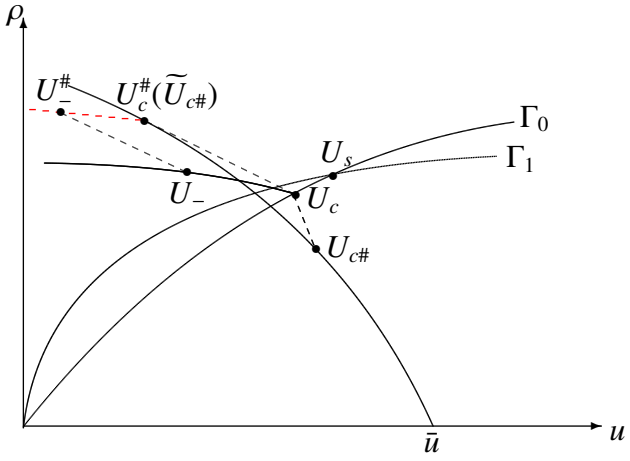


Figure 11. Case 2.1. $U_- \in D_1$, $u_c < u_s$.

Case 2.1.1. $u_{c\#} < u_+ < \bar{u}$. Denote

$$J(U_+, U) \cap R(U, U_{c\#}) = \{U_{n1}\},$$

and the Riemann solution is (see Figure 12(a))

$$R(U_c, U_-) \to S_0(U_{c\#}, U_c) \to R(U_{n1}, U_{c\#}) \to J(U_+, U_{n1}).$$

Case 2.1.2. $\widetilde{u}_{c\#} < u_+ < u_{c\#}$. Denote

$$J(U_+, U) \cap S(U, U_{c\#}) = \{U_{n2}\},$$

and the Riemann solution is (see Figure 12(b))

$$R(U_c, U_-) \to S_0(U_{c\#}, U_c) \to S(U_{n2}, U_{c\#}) \to J(U_+, U_{n2}).$$

Case 2.1.3. $u_+ > \bar{u}$. Denote $J(U_+, U) \cap \{\rho = 0\} = \{M\}$, and the Riemann solution is (see Figure 12(c))

$$R(U_c, U_-) \to S_0(U_{c\#}, U_c) \to R(\bar{U}, U_{c\#}) \to \text{Vacuum} \to J(U_+, M).$$

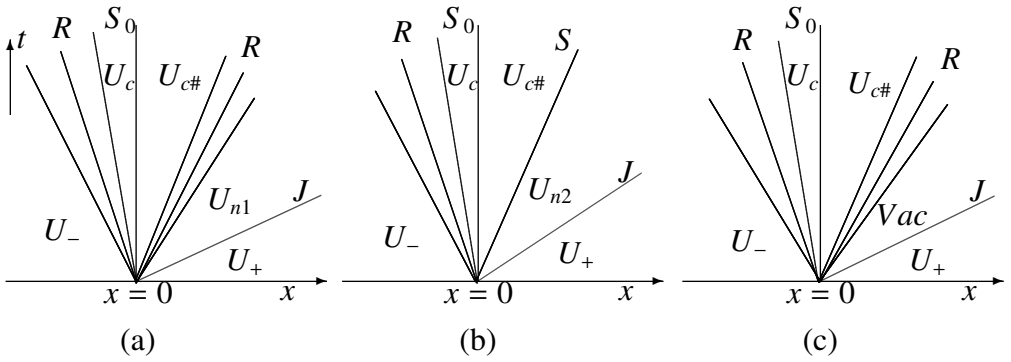


Figure 12. Case 2.1.1–2.1.3. (a) $u_{c\#} < u_+ < \bar{u}$; (b) $\widetilde{u}_{c\#} < u_+ < u_{c\#}$; (c) $u_+ > \bar{u}$.

Case 2.1.4. Let U_c jump to $U_c^\# \in D_1$ by a stationary wave. From any point $U_0 \in S(U, U_-) \cup R(U, U_-)$, $\rho > \rho_c$, a stationary wave jumps from U_0 to some state $U_0^\# \in D_1$, and such states form the curve $S_0(U_0^\#, U_0)$.

(1) If $0 < u_+ < u_-^\#$: denote $J(U_+, U) \cap S_0(U_0^\#, U_0) = \{U_{k1}^\#\}$, and $U_{k1}^\#$ is jumped by the stationary wave $S_0(U_{k1}^\#, U_{k1})$, where $U_{k1} \in S(U, U_-)$. The Riemann problem in this case is (see Figure 13(a))

$$S(U_{k1}, U_-) \to S_0(U_{k1}^\#, U_{k1}) \to J(U_+, U_{k1}^\#).$$

(2) If $u_-^\# < u_+ < u_c^\#$: denote $J(U_+, U) \cap S_0(U_0^\#, U_0) = \{U_{k2}^\#\}$, and $U_{k2}^\#$ is jumped by the stationary wave $S_0(U_{k2}^\#, U_{k2})$, where $U_{k2} \in R(U, U_-)$. The Riemann problem in this case is (see Figure 13(b))

$$R(U_{k2}, U_-) \to S_0(U_{k2}^\#, U_{k2}) \to J(U_+, U_{k2}^\#).$$

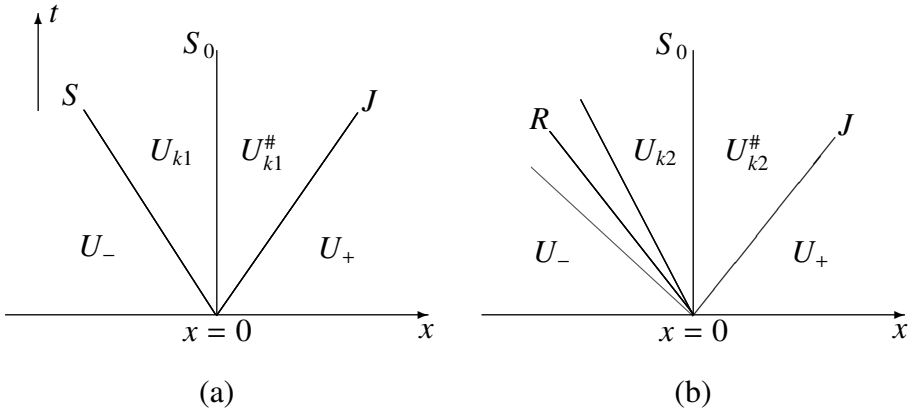


Figure 13. Case 2.1.4. (a) $0 < u_+ < u_-^\#$; (b) $u_-^\# < u_+ < u_c^\#$.

Case 2.2. $u_c > u_s$. From Lemma 6, we consider that $U_{c\#} \in D_2$, see Figure 14. Then, the Riemann solution is the same as in Case 2.1.

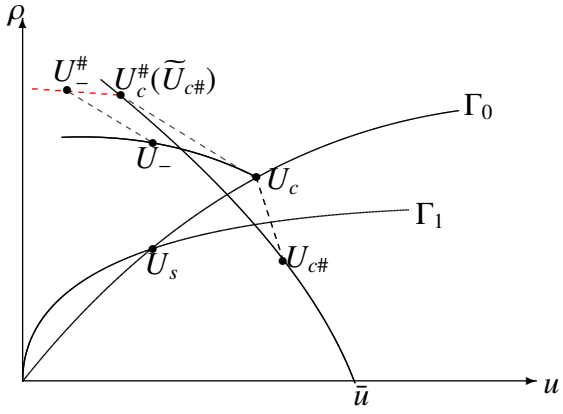


Figure 14. Case 2.2. $U_- \in D_1$; $u_c > u_s$; $U_{c\#} \in D_2$.

Case 3. $U_- \in D_3$. See Figure 15(a). The Riemann solution is the same as in Case 2.1.

Case 4. $U_- \in D_4$. From Lemma 6, the point $U_{-\#}$ may lie in D_2 or D_4, and in this case, we only consider that $U_{-\#} \in D_2$, see Figure 15(). Then, the Riemann solution is the same as in Case 1.

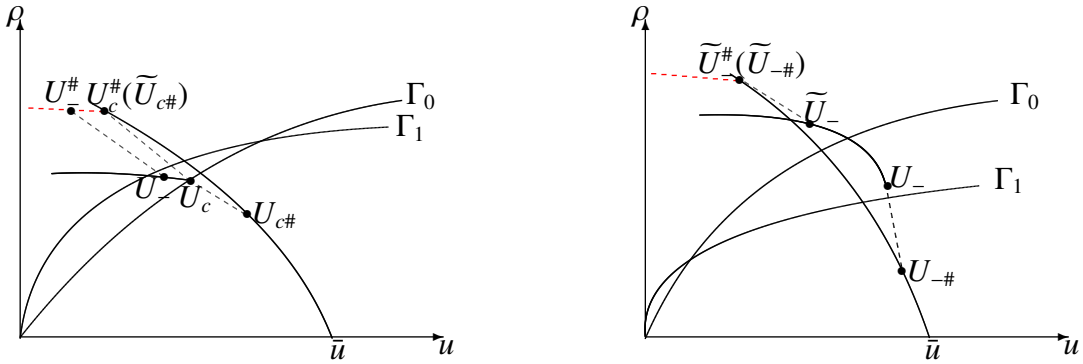


Figure 15. (a) Case 3: $U_- \in D_3$; (b) Case 4: $U_- \in D_4$.

4. Interaction of elementary waves with the stationary wave

In this section, we analyze interactions among elementary waves, focusing specifically on the interactions between the rarefaction waves, shock waves, and contact discontinuities with the stationary wave. It should be emphasized that a stationary wave generally changes with the road-condition parameter. Therefore, after crossing a stationary wave, the resulting state belongs to a different subsystem and all subsequent rarefaction curves, shock curves, characteristic speeds, and wave interactions are constructed using the new value of γ. We equip system (2.1) with the initial value problem of three piecewise constant data:

$$(u,\rho,\gamma)|_{t=0} = \begin{cases} U_- = (u_-,\rho_-,\gamma_0), & x < x_1, \\ U_m = (u_m,\rho_m,\gamma_0), & x_1 < x < x_2, \\ U_+ = (u_+,\rho_+,\gamma_1), & x > x_2. \end{cases} \tag{4.1}$$

4.1. The interaction of the rarefaction wave with the stationary wave

In this case, we consider the initial data (4.1), which satisfies

$$U_m \in R(U, U_-), \quad U_+ \in S_0(U, U_m).$$

Moreover, assume that $U_0 \in R(U, U_-)$ ($\rho_m \le \rho_0 \le \rho_-$), which jumps to U_1 via a stationary wave. We have the following equations:

$$\begin{cases} R(U, U_-) = R(U_m, U) : u_- + \left(\dfrac{1}{\rho_-} - \dfrac{1}{\rho^*}\right)^{-\gamma_0} = u_m + \left(\dfrac{1}{\rho_m} - \dfrac{1}{\rho^*}\right)^{-\gamma_0}, \\ S_0(U_1, U_0) : \begin{cases} \rho_0 u_0 = \rho_1 u_1, \\ u_0 + \left(\dfrac{1}{\rho_0} - \dfrac{1}{\rho^*}\right)^{-\gamma_0} = u_1 + \left(\dfrac{1}{\rho_1} - \dfrac{1}{\rho^*}\right)^{-\gamma_1}. \end{cases} \end{cases} \tag{4.2}$$

We define an auxiliary curve $S_0(U_1, U_0)$, which represents the stationary solution U_1 from a given left-hand state $U_0 \in R(U, U_-)$. From (4.2), the expression for the curve $S_0(U_1, U_0)$ is

$$u_1 + \left(\frac{1}{\rho_1} - \frac{1}{\rho^*}\right)^{-\gamma_1} = u_0 + \left(\frac{1}{\rho_0} - \frac{1}{\rho^*}\right)^{-\gamma_0} = u_- + \left(\frac{1}{\rho_-} - \frac{1}{\rho^*}\right)^{-\gamma_0}.$$

Thus, $S_0(U_1, U_0)$ is a decreasing curve, as

$$\frac{\mathrm{d}u_1}{\mathrm{d}\rho_1} = -\frac{\gamma_1}{\rho_1^2}\left(\frac{1}{\rho_1} - \frac{1}{\rho^*}\right)^{-\gamma_1 - 1} < 0.$$

Moreover, $S_0(U_1, U_0)$ passes through U_+ since U_m and U_+ are connected by a stationary wave. Thus, $S_0(U_1, U_0)$ is on the left of $J(U, U_+)$ since S_0 is a decreasing curve.

The long-time behavior of the solution is given by

$$R(U_m, U_-) \triangleright S_0(U_+, U_m) \to S_0(U_{-\#}, U_-) \triangleright R(U_5, U_{-\#}) \triangleright J(U_+, U_5),$$

where $\triangleright$ denotes "follows." The result is illustrated in Figure 16.

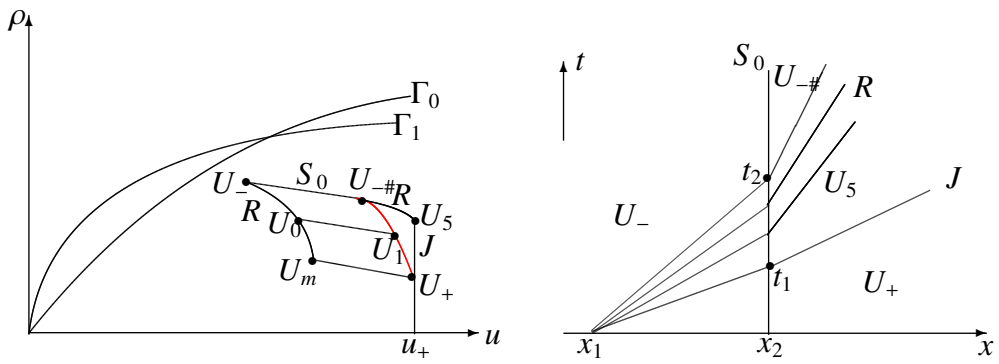


Figure 16. The result of the rarefaction wave interacts with the stationary wave.

4.2. The interaction of the shock wave with the stationary wave

In this case, we have $U_m \in S(U, U_-)$ and $U_+ \in S_0(U, U_m)$. We have

$$\begin{cases} S(U_m, U_-) : u_- + \left(\frac{1}{\rho_-} - \frac{1}{\rho^*}\right)^{-\gamma_0} = u_m + \left(\frac{1}{\rho_m} - \frac{1}{\rho^*}\right)^{-\gamma_0}, \\ S_0(U_+, U_m) : \begin{cases} \rho_m u_m = \rho_+ u_+, \\ u_m + \left(\frac{1}{\rho_m} - \frac{1}{\rho^*}\right)^{-\gamma_0} = u_+ + \left(\frac{1}{\rho_+} - \frac{1}{\rho^*}\right)^{-\gamma_1}. \end{cases} \end{cases} \tag{4.3}$$

Since the propagation speed of the shock is given by

$$\sigma(U_m, U_-) = u_m + \frac{\rho_- \left(\left(\frac{1}{\rho_-} - \frac{1}{\rho^*}\right)^{-\gamma_0} - \left(\frac{1}{\rho_m} - \frac{1}{\rho^*}\right)^{-\gamma_0}\right)}{\rho_m - \rho_-},$$

which is positive, this implies that the curve $S(U_m, U_-)$ will overtake the curve S_0. Similarly, we define the curve $S_0(U_1, U_0)$, formulated by U_1, where $U_0 \in S(U, U_-)$. Since the rarefaction wave curve and the shock wave curve have the same form, we conclude that $S_0(U_1, U_0)$ is also monotonically decreasing. As a result, $S_0(U_1, U_0)$ is on the right side of $J(U, U_+)$.

The large-time behavior of the solution is represented as (see Figure 17)

$$S(U_m, U_-) \triangleright S_0(U_+, U_m) \to S_0(U_{-\#}, U_-) \triangleright S(U_6, U_{-\#}) \triangleright J(U_+, U_6).$$

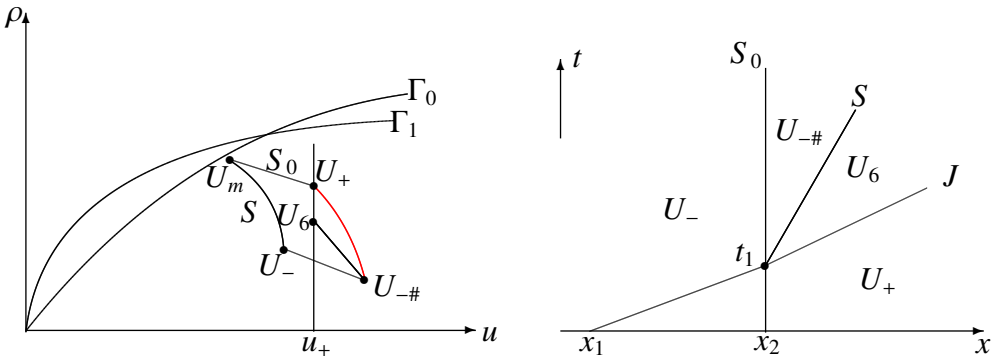


Figure 17. The result of a shock wave interacting with a stationary wave.

4.3. The interaction of the contact discontinuity with the stationary wave

Consider $U_m \in J(U, U_-), U_+ \in S_0(U, U_m)$, where the contact discontinuity has a positive speed $\sigma(U_m, U_-) = u_m > 0$, which indicates that it will overtake the stationary wave at some finite time. The equations governing the system are

$$\begin{cases} J(U, U_-) : u = u_-, (\rho \neq \rho_-), \\ S_0(U_1, U_0) : \begin{cases} \rho_0 u_0 = \rho_1 u_1, \\ u_0 + \left(\frac{1}{\rho_0} - \frac{1}{\rho^*}\right)^{-\gamma_0} = u_1 + \left(\frac{1}{\rho_1} - \frac{1}{\rho^*}\right)^{-\gamma_1}. \end{cases} \end{cases} \tag{4.4}$$

Since $U_0 \in J(U, U_-)$ indicates $u_0 = u_-$, by differentiating (4.4), we obtain

$$\begin{cases} u_0 \mathrm{d}\rho_0 = \rho_1 \mathrm{d}u_1 + u_1 \mathrm{d}\rho_1 \\ \dfrac{\gamma_0}{\rho_0^2}\left(\dfrac{1}{\rho_0} - \dfrac{1}{\rho^*}\right)^{-\gamma_0 - 1} \mathrm{d}\rho_0 = \mathrm{d}u_1 + \dfrac{\gamma_1}{\rho_1^2}\left(\dfrac{1}{\rho_1} - \dfrac{1}{\rho^*}\right)^{-\gamma_1 - 1} \mathrm{d}\rho_1. \end{cases} \tag{4.5}$$

For the above equation, we eliminate $\mathrm{d}\rho_0$ and determine the monotone property of the curve $S_0(U_1, U_0)$ as follows:

$$\frac{\mathrm{d}u_1}{\mathrm{d}\rho_1} = \frac{\frac{u_0}{\rho_1}\left[\frac{\gamma_0}{\rho_0}\left(\frac{1}{\rho_0} - \frac{1}{\rho^*}\right)^{-\gamma_0 - 1} - \frac{\gamma_1}{\rho_1}\left(\frac{1}{\rho_1} - \frac{1}{\rho^*}\right)^{-\gamma_1 - 1}\right]}{u_0 - \frac{u_0}{u_1}\frac{\gamma_0}{\rho_0}\left(\frac{1}{\rho_0} - \frac{1}{\rho^*}\right)^{-\gamma_0 - 1}}. \tag{4.6}$$

Since $U_0 \in D_1 \cup D_2 \cup D_3 \cup D_4$, the state U_0 does not lie on the critical curves Γ_0 or Γ_1. Hence the resonance condition $\lambda_1 = \lambda_3 = 0$ cannot occur, and the denominator in (4.6) is nonzero. Now we discuss the curve $u_1(\rho_1)$ defined in (4.4) in the (u, ρ) plane.

First, when $U_0 \in \{D_1 \cup D_3\}$, this implies

$$u_0 < \frac{\gamma_0}{\rho_0}\left(\frac{1}{\rho_0} - \frac{1}{\rho^*}\right)^{-\gamma_0 - 1}.$$

Furthermore, from the curve of S_0, see Figure 3, we have $u_1 < u_0, \rho_1 > \rho_0$. Thus, the denominator of (4.6) is

$$u_0 - \frac{u_0}{u_1}\frac{\gamma_0}{\rho_0}\left(\frac{1}{\rho_0} - \frac{1}{\rho^*}\right)^{-\gamma_0 - 1} < 0. \tag{4.7}$$

From the third equation of (4.4), we have

$$\left(\frac{1}{\rho_0} - \frac{1}{\rho^*}\right)^{-\gamma_0 - 1} = \frac{\rho_0 \rho^*}{\rho^* - \rho_0}\left((u_1 - u_0) + \left(\frac{1}{\rho_1} - \frac{1}{\rho^*}\right)^{-\gamma_1}\right),$$

so the numerator of (4.6) can be transformed into

$$\frac{u_0}{\rho_1}\left[(u_1 - u_0)\frac{\rho_0 \rho^*}{\rho^* - \rho_0} + \frac{1}{\rho_1}\left(\gamma_0 \frac{\rho^* - \rho_1}{\rho^* - \rho_0} - \gamma_1\right)\left(\frac{1}{\rho_1} - \frac{1}{\rho^*}\right)^{-\gamma_1 - 1}\right]. \tag{4.8}$$

Since $u_1 - u_0 < 0$, $\rho^* - \rho_1 < \rho^* - \rho_0$, and $\gamma_1 > \gamma_0$, the above formula is negative. Then, the numerator of (4.6) is

$$\frac{u_0}{\rho_1}\left[\frac{\gamma_0}{\rho_0}\left(\frac{1}{\rho_0} - \frac{1}{\rho^*}\right)^{-\gamma_0 - 1} - \frac{\gamma_1}{\rho_1}\left(\frac{1}{\rho_1} - \frac{1}{\rho^*}\right)^{-\gamma_1 - 1}\right] < 0.$$

Therefore, we conclude that

$$\frac{\mathrm{d}u_1}{\mathrm{d}\rho_1} > 0.$$

When $U_0 \in \{D_2 \cup D_4\}$, similarly, we have

$$u_0 > \frac{\gamma_0}{\rho_0}\left(\frac{1}{\rho_0} - \frac{1}{\rho^*}\right)^{-\gamma_0 - 1}$$

and $u_1 > u_0, \rho_1 < \rho_0$. Thus, the denominator of (4.6) is

$$u_0 - \frac{u_0}{u_1}\frac{\gamma_0}{\rho_0}\left(\frac{1}{\rho_0} - \frac{1}{\rho^*}\right)^{-\gamma_0-1} > 0.$$

Now, we determine the sign of the numerator of (4.6). Denote

$$G(\rho, \gamma) = \frac{\gamma}{\rho}\left(\frac{1}{\rho} - \frac{1}{\rho^*}\right)^{-\gamma-1},$$

and taking the partial derivatives of $G(\rho, \gamma)$ with respect to ρ and γ, we get

$$\frac{\partial G}{\partial \rho} = \frac{\gamma}{\rho^2}\left(\frac{\rho + \gamma\rho^*}{\rho^* - \rho}\right)\left(\frac{1}{\rho} - \frac{1}{\rho^*}\right)^{-\gamma-1}, \tag{4.9}$$

$$\frac{\partial G}{\partial \gamma} = \frac{1}{\rho}\left(1 - \gamma \ln\left(\frac{1}{\rho} - \frac{1}{\rho^*}\right)\right)\left(\frac{1}{\rho} - \frac{1}{\rho^*}\right)^{-\gamma-1}. \tag{4.10}$$

By Taylor expansion, we have

$$G(\rho_1, \gamma_1) = G(\rho_0, \gamma_0) + \frac{\partial G(\xi)}{\partial \rho}\frac{\mathrm{d}\rho}{\mathrm{d}\gamma}(\gamma_1 - \gamma_0) + \frac{\partial G(\xi)}{\partial \gamma}(\gamma_1 - \gamma_0) + O((\gamma_1 - \gamma_0)^2) \tag{4.11}$$

$$= G(\rho_0, \gamma_0) + \left(\frac{\partial G(\xi)}{\partial \rho}\frac{\mathrm{d}\rho}{\mathrm{d}\gamma} + \frac{\partial G(\xi)}{\partial \gamma}\right)(\gamma_1 - \gamma_0) + O((\gamma_1 - \gamma_0)^2), \tag{4.12}$$

where $\mathrm{d}\rho/\mathrm{d}\gamma$ is defined in (2.11). To simplify the calculations, we only consider the case where γ_1 is very close to γ_0, meaning that $\gamma_1 - \gamma_0$ is sufficiently small. Thus, the value of $G(\rho_1, \gamma_0)$ is mainly determined by the first two parts. Since $\partial G/\partial \rho > 0$, $\mathrm{d}\rho/\mathrm{d}\gamma < 0$ and $\gamma_1 - \gamma_0 > 0$. If $\partial G/\partial \gamma > 0$, we can not determine the sign of $\mathrm{d}u_1/\mathrm{d}\rho_1$. For definiteness and simplicity, we assume that $\partial G/\partial \gamma < 0$, which requires that

$$\ln\left(\frac{1}{\rho} - \frac{1}{\rho^*}\right) > \frac{1}{\gamma}.$$

Consequently, we conclude that $G(\rho_1, \gamma_1) < G(\rho_0, \gamma_0)$. Hence, the numerator of (4.6) is positive. Combining this with (4.7), we can infer that $\mathrm{d}u_1/\mathrm{d}\rho_1 > 0$.

Remark 7. The above argument holds for sufficiently small variation of $|\gamma_1 - \gamma_0|$. The sign of $\partial G/\partial \gamma$ is related to the expression

$$1 - \gamma \ln\left(\frac{1}{\rho} - \frac{1}{\rho^*}\right),$$

which may change sign depending on the parameters. For

$$\ln\left(\frac{1}{\rho} - \frac{1}{\rho^*}\right) < \frac{1}{\gamma},$$

the sign of $\mathrm{d}u_1/\mathrm{d}\rho_1$ may not be determined. A global investigation for arbitrary values of $\gamma_1 - \gamma_0$ is left for future work.

In conclusion, we have

$$\frac{\mathrm{d}u_1}{\mathrm{d}\rho_1} > 0, \quad U_0 \in \{D_1 \cup D_2 \cup D_3 \cup D_4\}, \tag{4.13}$$

which means that the stationary wave is an increasing curve in the whole (u, ρ) plane, which is used to define some critical points and classify the interaction results. Based on the above conclusion, we will now proceed by examining each specific case individually.

Case 1. $U_+ \in \{D_2 \cup D_4\}$. From the assumption, U_m and U_+ are connected by a stationary wave.

We now define some critical points before discussing the interaction results. First, denote $U_c = J(U, U_-) \cap \Gamma_0$, and U_c jumps to $U_{c\#} \in D_2$ by a stationary wave. Since the curve $S_0(U_1, U_0)$ passes through U_+ and increases from $(u_-, 0)$ to $U_{c\#}$ from (4.13), we draw $R((u_+, 0), U)$, which intersects with $S_0(U_1, U_0)$ at $\widetilde{U}_\#$. $\widetilde{U}_\#$ is obtained by a stationary jump from $\widetilde{U} \in \{(u, \rho)|u = u_-\}$.

Moreover, for any point $U_{c_0} \in \Gamma_0$ with $\rho_{c_0} > \rho_c$, it jumps to $U_{c_1} \in D_2$, and such states U_{c_1} can form a curve denoted by $S_0(U_{c_1}, U_{c_0})$. From Eq (3.6), we know that the curve is increasing. Denote $\bar{U} \in \{(u, \rho)|u = u_+\}$, which satisfies that $\sigma(\bar{U}, U^s_{c\#}) = 0$. From Lemma 4, we know that $\bar{U}$ and $U_c^{s\#}$ coincide, where $U_c^{s\#} \in D_1$ and U_c^s are also connected by a stationary wave. We draw the curve $R(U, U_c^s)$, which intersects $\{(u, \rho)|u = u_-\}$ at U^s, see Figure 18. After defining these critical points, we now discuss the interaction results as follows.

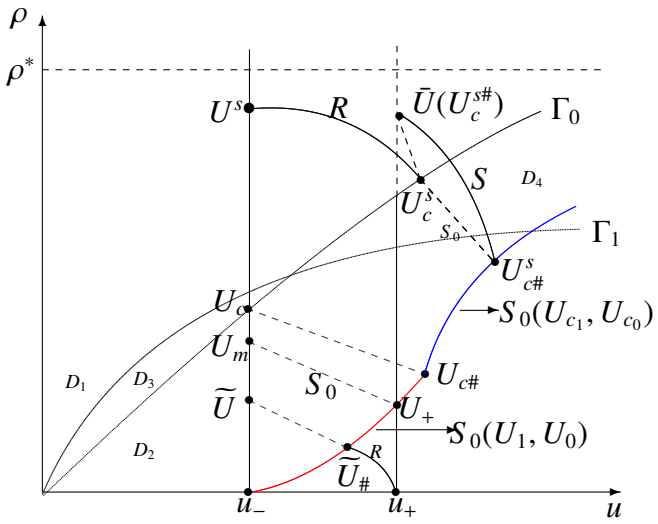


Figure 18. Case 1. $U_+ \in D_2 \cup D_4$.

Case 1.1. $0 < \rho_- < \rho_m$. In this case, if $\widetilde{\rho} < \rho_- < \rho_m$, U_- will first jump to $U_{-\#}$ by a stationary wave, and then $U_{-\#}$ will reach to U_3 by $R(U_3, U_{-\#})$, where $u_3 = u_+$. Finally, U_3 reaches U_+ by $J(U_+, U_3)$. That is,

$$J(U_m, U_-) \triangleright S_0(U_+, U_m) \to S_0(U_{-\#}, U_-) \triangleright R(U_3, U_{-\#}) \triangleright J(U_+, U_3).$$

Moreover, if $0 < \rho_- \leq \widetilde{\rho}$, there exists a vacuum state, and we denote $\{U_4\} = R(U_4, U_{-\#}) \cap \{\rho = 0\}$ and $U_5 = (u_+, 0)$. Then

$$J(U_m, U_-) \triangleright S_0(U_+, U_m) \to S_0(U_{-\#}, U_-) \triangleright R(U_4, U_{-\#}) \triangleright \text{Vacuum} \triangleright J(U_+, U_5).$$

Case 1.2. $\rho_m < \rho_- < \rho_c$. In this case, the solution starts with a stationary wave from U_- to $U_{-\#}$, then $U_{-\#}$ reaches U_3 by $S(U_3, U_{-\#})$ with positive speed, and finally, U_3 reaches U_+ by $J(U_+, U_3)$, that is,

$$J(U_m, U_-) \triangleright S_0(U_+, U_m) \to S_0(U_{-\#}, U_-) \triangleright S(U_3, U_{-\#}) \triangleright J(U_+, U_3).$$

Case 1.3. $\rho_c < \rho_- < \rho^s$. In this case, the solution starts with a rarefaction wave from U_- to $U_3 \in \Gamma_0$, and U_3 jumps to $U_{3\#} \in D_2$ by a stationary wave. Then, it is followed by a shock wave with positive speed from $U_{3\#}$ to U_4, and finally, U_4 gets to U_+ by $J(U_+, U_4)$, i.e.,

$$J(U_m, U_-) \triangleright S_0(U_+, U_m) \to R(U_3, U_-) \triangleright S_0(U_{3\#}, U_3) \triangleright S(U_4, U_{3\#}) \triangleright J(U_+, U_4).$$

Case 1.4. $\rho^s < \rho_- < \rho^*$. The solution U_- gets to $U_3 \in D_1$ first by a rarefaction wave, then jumps to $U_3^\#$ by a stationary wave, followed by a contact discontinuity $J(U_+, U_3^\#)$, i.e.,

$$J(U_m, U_-) \triangleright S_0(U_+, U_m) \to R(U_3, U_-) \triangleright S_0(U_3^\#, U_3) \triangleright J(U_+, U_3^\#).$$

Case 2. $U_+ \in D_1 \cup D_3$. In this case, $U_m \in D_1$. First, let $U_c = J(U, U_-) \cap \Gamma_0$, and then U_c jumps to $U_c^\# \in D_1$ by a stationary wave. The curve $S_0(U_1, U_0)$ passes through U_+ and increases in D_1 from (4.13) with $\rho_1 > \rho_c^\#$, and U_+ jumps from $U_m \in \{(u, \rho) | u = u_-\}$ by $S_0(U_+, U_m)$. There exists a point $U_{c\#}$ that jumped from U_c by a stationary wave. We then draw the curve $S(\widetilde{U}_{c\#}, U_{c\#})$, where the point $\widetilde{U}_{c\#}$ coincides with $U_c^\#$, according to Lemma 4. For any point $U_0 \in \{(u, \rho) | u = u_-\}$ with $\rho_0 < \rho_c$, which jumps to $U_1 \in S_0(U_1, U_0)$, there exists $\widetilde{U}_1 \in D_1$. Hence, we obtain an increasing curve $S(\widetilde{U}_1, U_1)$, see Figure 19, We now discuss the interaction results as follows by using the critical points.

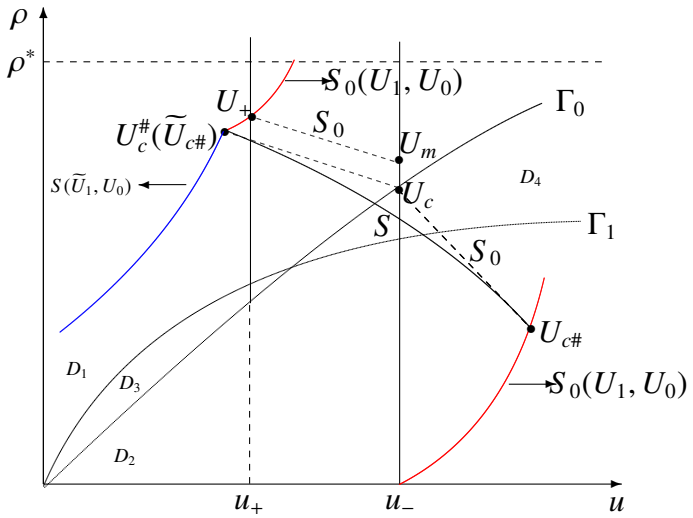


Figure 19. Case 2. $U_+ \in D_1 \cup D_3$.

Case 2.1. $0 < \rho_- < \rho_c$. In this case, U_- first jumps to $U_{-\#}$ by a stationary wave, followed by a shock wave from $U_{-\#}$ to $U_3 \in J(U_+, U)$ with positive speed, and then followed by a contact discontinuity from U_3 to U_+, that is,

$$J(U_m, U_-) \triangleright S_0(U_+, U_m) \to S_0(U_{-\#}, U_-) \triangleright S(U_3, U_{-\#}) \triangleright J(U_+, U_3).$$

Case 2.2. $\rho_c < \rho_- < \rho_m$. The result in this case is U_- starting with a rarefaction wave to $U_3 \in \Gamma_0$, followed by a stationary wave to $U_{3\#}$, then followed by a shock wave to $U_4 \in J(U_+, U)$ with positive speed, and jumping to U_+ by a contact discontinuity, i.e.,

$$J(U_m, U_-) \triangleright S_0(U_+, U_m) \to R(U_3, U_-) \triangleright S_0(U_{3\#}, U_3) \triangleright S(U_4, U_{3\#}) \triangleright J(U_+, U_4).$$

Case 2.3. $\rho_m < \rho_- < \rho^*$. The solution U_- gets to $U_3 \in D_1$ by a shock wave, then jumps to $U_3^\# \in J(U_+, U)$ by a stationary wave, followed by a contact discontinuity $J(U_+, U_3^\#)$, i.e.,

$$J(U_m, U_-) \triangleright S_0(U_+, U_m) \to S(U_3, U_-) \triangleright S_0(U_3^\#, U_3) \triangleright J(U_+, U_3^\#).$$

5. Numerical tests

In this section, we present numerical simulations of the Riemann solution for system (2.1) to demonstrate our analysis. The numerical method consists of a stationary-state reconstruction followed by a finite volume Lax–Friedrichs method. At each time step, we first reconstruct the stationary states at the cell interfaces to account for the discontinuity of the road-condition parameter γ. Specifically, for each interface, two intermediate states are computed by solving the stationary-wave relations. For example, the left reconstructed state $U_{j+1,-}$ is obtained from the right state U_{j+1} through

$$\begin{cases} \rho_{j+1,-} u_{j+1,-} = \rho_{j+1} u_{j+1}, \\ u_{j+1,-} + \left(\dfrac{1}{\rho_{j+1,-}} - \dfrac{1}{\rho^*}\right)^{-\gamma_j} = u_{j+1} + \left(\dfrac{1}{\rho_{j+1}} - \dfrac{1}{\rho^*}\right)^{-\gamma_{j+1}}, \end{cases} \tag{5.1}$$

while the right reconstructed state $U_{j-1,+}$ is obtained analogously.

After the stationary-state reconstruction, the conserved variables are updated by a finite volume Lax–Friedrichs scheme,

$$U_j^{n+1} = U_j^n - \frac{\Delta t}{\Delta x}\left[g_N(U_j^n, U_{j+1,-}^n) - g_N(U_{j-1,+}^n, U_j^n)\right], \tag{5.2}$$

where the numerical flux is given by

$$g_N(U, V) = \frac{1}{2}(F(U) + F(V)) - \frac{\Delta x}{2\Delta t}(V - U). \tag{5.3}$$

The stationary-state reconstruction enables the numerical scheme to preserve the stationary discontinuity induced by the spatial variation of γ. For all numerical tests, the computational domain is taken as $[0, 50]$ and discretized into 3000 uniform cells. The road condition, represented by the parameter γ, is assumed to change at $x = 25$. The maximal density is fixed as $\rho^* = 120$. The time step is determined by the Courant–Friedrichs–Lewy (CFL) condition with a CFL number 0.6.

Test 1. The initial data is given as follows:

$$\begin{cases} U_- = (u_-, \rho_-, \gamma_0) = (3.0, 0.7, 1.7), & x < 25, \\ U_+ = (u_+, \rho_+, \gamma_1) = (3.0, 0.8, 2.5), & x > 25. \end{cases} \tag{5.4}$$

The output time is $t = 2$ and the solution is shown in Figure 20. The Riemann solution consists of a stationary wave S_0, followed by a shock wave S, and then a contact discontinuity J, with the detailed solution illustrated in Figure 9(a). This case corresponds to Case 1.1. The numerical result is the same as in the analysis.

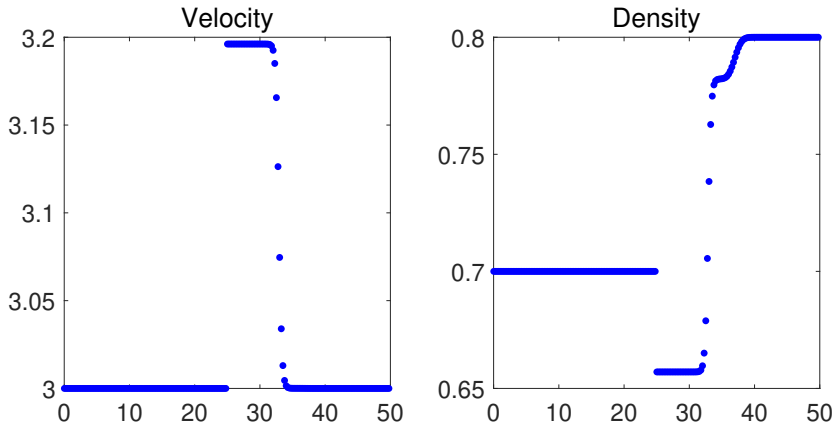


Figure 20. Test 1: The solution for velocity and density at $t = 2$.

Test 2. The initial data is given as follows:

$$\begin{cases} U_- = (u_-, \rho_-, \gamma_0) = (6.0, 5.0, 1.2), & x < 25, \\ U_+ = (u_+, \rho_+, \gamma_1) = (3.0, 4.7, 1.3), & x > 25. \end{cases} \tag{5.5}$$

The output time is $t = 1$ and the solution is shown in Figure 21. The Riemann solution consists of a shock wave S, followed by a stationary wave S_0, and then a contact discontinuity J, with the detailed solution illustrated in Figure 10. This case corresponds to Case 1.4. The result matches well with our analysis.

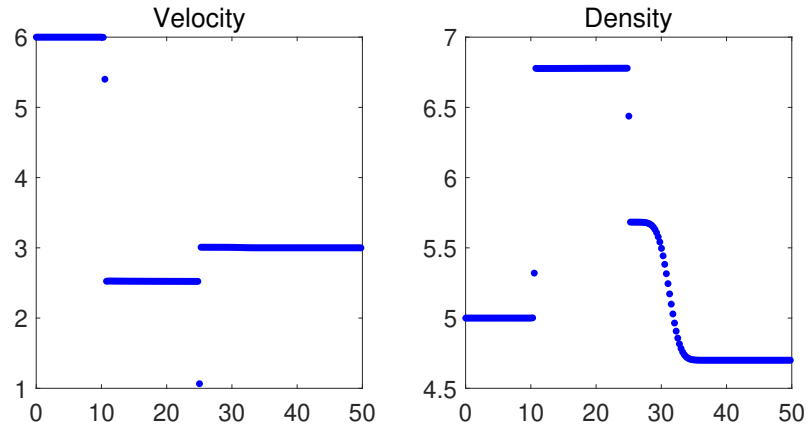


Figure 21. Test 2: The solution for velocity and density at $t = 1$.

Test 3. The initial data is given as follows:

$$U(x,0) = \begin{cases} U_- = (u_-, \rho_-, \gamma_0) = (0.5, 1.2, 1.2), & x < 25, \\ U_+ = (u_+, \rho_+, \gamma_1) = (1.0, 0.7, 2.0), & x > 25. \end{cases} \tag{5.6}$$

The output time is $t = 5$ and the solution is shown in Figure 22. The Riemann solution consists of a rarefaction wave R, which coincides with a stationary wave S_0, followed by a shock wave S, and a contact discontinuity J, with the detailed solution illustrated in Figure 12(b). This case corresponds to Case 2.1.2. The result is consistent with our analysis.

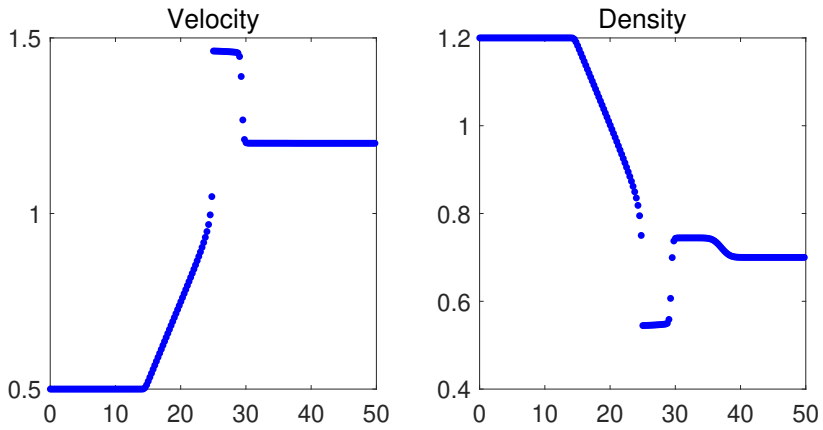


Figure 22. Test 3: The solution for velocity and density at $t = 5$.

Test 4. The initial data is given as follows:

$$U(x,0) = \begin{cases} U_- = (u_-, \rho_-, \gamma_0) = (0.5, 1.3, 2.0), & x < 25, \\ U_+ = (u_+, \rho_+, \gamma_1) = (6.0, 0.3, 8.0), & x > 25. \end{cases} \tag{5.7}$$

The output time is $t = 1.5$ and the solution is shown in Figure 23. The Riemann solution consists of a rarefaction wave R that coincides with a stationary wave S_0, followed by another rarefaction wave R connecting to a vacuum state, and then a contact discontinuity J, with the detailed solution illustrated in Figure 12(c). This case corresponds to Case 2.1.3. The result is consistent with our analysis.

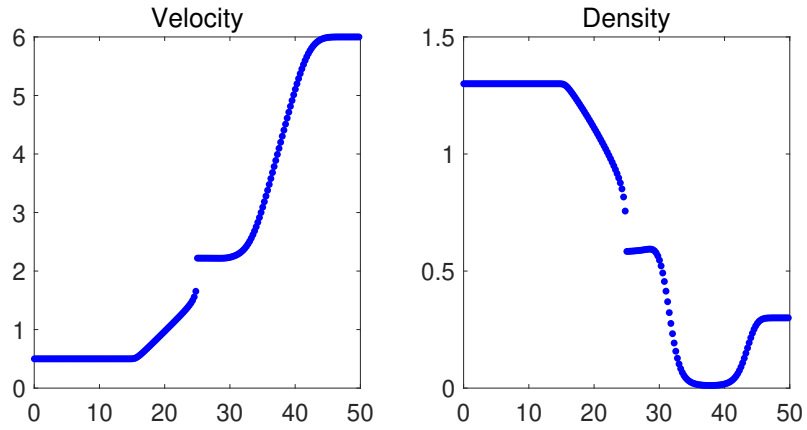


Figure 23. Test 4: The solution for velocity and density at $t = 1.5$.

Test 5. The initial data is given as follows:

$$U(x,0) = \begin{cases} U_- = (u_-, \rho_-, \gamma_0) = (5.0, 4.0, 1.8), & x < 25, \\ U_+ = (u_+, \rho_+, \gamma_1) = (8.0, 3.0, 1.9), & x > 25. \end{cases} \tag{5.8}$$

The output time is $t = 0.5$ and the solution is shown in Figure 24. The Riemann solution consists of a rarefaction wave R, followed by a stationary wave S_0, and then a contact discontinuity J, with the detailed solution illustrated in Figure 13(b). This case corresponds to Case 2.1.4. The result is consistent with our analysis.

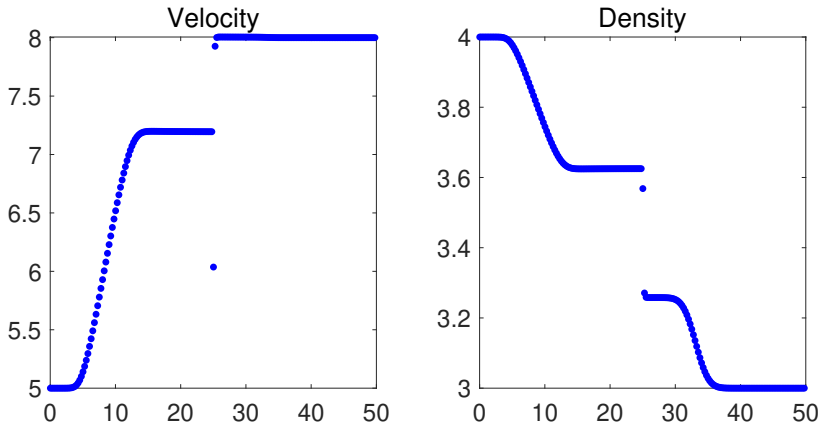


Figure 24. Test 5: The solution for velocity and density at $t = 0.5$.

6. Conclusions

In summary, we have investigated and extended the AR traffic flow model to account for varying road conditions, and have applied the method of characteristics to derive elementary waves, including rarefaction waves, shock waves, contact discontinuities, and stationary waves. Additionally, we have solved the Riemann problem comprehensively and explored the interaction results of rarefaction waves, shock waves, and contact discontinuities, respectively, with stationary waves. The results hopefully provide valuable insights into more complicated behaviors of traffic flow under different road conditions. Finally, we present numerical simulations under various initial conditions, which demonstrate the effectiveness of our model.

Author contributions

Shuzhi Liu: Conceptualization, mathematical analysis, review and editing; Yuanhong Wu: Computation, validation, numerical computation and verification, writing of the original draft. Both authors have read and approved the final version of the manuscript for publication.

Use of Generative-AI tools declaration

No Generative-AI tools were used in this paper.

Acknowledgments

Thanks to the anonymous reviewers' valuable suggestions, which makes this paper much better compared to the original version.

Conflict of interest

The authors declare no conflicts of interest in this paper.

References

1. A. Aw, M. Rascle, Resurrection of "second order" models of traffic flow, *SIAM J. Appl. Math.*, **60** (2000), 916–938. https://doi.org/10.1137/S0036139997332099
2. C. F. Daganzo, Requiem for second-order fluid approximations of traffic flow, *Transp. Res. Part B Methodol.*, **29** (1995), 277–286. https://doi.org/10.1016/0191-2615(95)00007-Z
3. H. M. Zhang, A non-equilibrium traffic model devoid of gas-like behavior, *Transp. Res. Part B Methodol.*, **36** (2002), 275–290. https://doi.org/10.1016/S0191-2615(00)00050-3
4. W. F. Jiang, Z. Wang, Developing an Aw–Rascle model of traffic flow, *J. Eng. Math.*, **97** (2016), 135–146. https://doi.org/10.1007/s10665-015-9801-2
5. Z. Shao, The Riemann problem for a traffic flow model, *Phys. Fluids*, **35** (2023), 036104. https://doi.org/10.1063/5.0141732
6. C. Shen, M. Sun, Formation of delta shocks and vacuum states in the vanishing pressure limit of Riemann solutions to the perturbed Aw–Rascle model, *J. Differ. Equations*, **249** (2010), 3024–3051. https://doi.org/10.1016/j.jde.2010.09.004
7. G. Yin, J. Chen, Existence and stability of Riemann solution to the Aw–Rascle model with friction, *Indian J. Pure Appl. Math.*, **49** (2018), 671–688. https://doi.org/10.1007/s13226-018-0294-3
8. M. Sun, Interactions of elementary waves for the Aw–Rascle model, *SIAM J. Appl. Math.*, **69** (2009), 1542–1558. https://doi.org/10.1137/080731402
9. X. Xin, M. Sun, The vanishing pressure limits of Riemann solutions for the Aw–Rascle hydrodynamic traffic flow model with the logarithmic equation of state, *Chaos Solitons Fract.*, **181** (2024), 114671. https://doi.org/10.1016/j.chaos.2024.114671
10. J. M. Greenberg, Extensions and amplifications of a traffic model of Aw and Rascle, *SIAM J. Appl. Math.*, **62** (2002), 729–745. https://doi.org/10.1137/S0036139900378657
11. M. Herty, M. Rascle, Coupling conditions for a class of second-order models for traffic flow, *SIAM J. Math. Anal.*, **38** (2006), 595–616. https://doi.org/10.1137/05062617X
12. Y. Wu, S. Liu, Q. Zhang, A constrained Aw–Rascle-type traffic flow model: formulation and numerical validation, *Appl. Math. Comput.*, **531** (2026), 130171. https://doi.org/10.1016/j.amc.2026.130171
13. F. Berthelin, P. Degond, M. Delitala, M. Rascle, A model for the formation and evolution of traffic jams, *Arch. Ration. Mech. Anal.*, **187** (2008), 185–220. https://doi.org/10.1007/s00205-007-0061-9

14. F. Berthelin, P. Degond, V. Le Blanc, S. Moutari, M. Rascle, J. Royer, A traffic-flow model with constraints for the modeling of traffic jams, *Math. Models Methods Appl. Sci.*, **18** (2008), 1269–1298. https://doi.org/10.1142/S0218202508003030

15. Y. Hu, G. Wang, The resonance behavior for the coupling of two Aw–Rascle traffic models, *Adv. Differ. Equ.*, **2020** (2020), 60. https://doi.org/10.1186/s13662-020-2502-9

16. P. G. LeFloch, M. D. Thanh, The Riemann problem for fluid flows in a nozzle with discontinuous cross-section, *Commun. Math. Sci.*, **1** (2003), 763–797. https://doi.org/10.4310/cms.2003.v1.n4.a6

17. N. Andrianov, G. Warnecke, The Riemann problem for the Baer–Nunziato two-phase flow model, *J. Comput. Phys.*, **195** (2004), 434–464. https://doi.org/10.1016/j.jcp.2003.10.006

18. W. Sheng, Q. Zhang, The Riemann problem for a traffic flow model on a road with variable widths, *IMA J. Appl. Math.*, **87** (2022), 757–785. https://doi.org/10.1093/imamat/hxac020

19. Y. Jia, Z. Si, Z. Ju, H. Feng, J. Zhang, X. Yan, et al., Convolutional-recurrent neural network for the prediction of formation and switching dynamics for multicolor solitons, *Sci. China Phys. Mech. Astron.*, **68** (2025), 284211. https://doi.org/10.1007/s11433-025-2679-8

20. J. P. Lebacque, S. Mammar, H. Haj-Salem, The Aw–Rascle and Zhang's model: vacuum problems, existence and regularity of the solutions of the Riemann problem, *Transp. Res. Part B Methodol.*, **41** (2007), 710–721. https://doi.org/10.1016/j.trb.2006.11.005

21. Y. Liu, B. Guo, D. Wang, Patterns of emergent nonlinear waves in an initial discontinuity problem of the bad Jaulent–Miodek equation, *Acta Math. Appl. Sin. Engl. Ser.*, **42** (2026), 582–607. https://doi.org/10.1007/s10255-024-1142-3

22. Y. Liu, S. Zeng, Structure and dynamic evolution of Riemann problem solutions for the Kundu equation with step-like initial data, *Nonlinear Dyn.*, **113** (2025), 12075–12097. https://doi.org/10.1007/s11071-024-10819-0

23. C. Shen, M. Sun, The Riemann problem for the one-dimensional isentropic Euler system under the body force with varying gamma law, *Physica D*, **448** (2023), 133731. https://doi.org/10.1016/j.physd.2023.133731

24. F. Wu, Y. Liu, Z. Yan, Classification and dynamic analysis of nonlinear wave structures evolving from initial discontinuities in the coupled Zakharov–Ito system, *Physica D*, **482** (2025), 134896. https://doi.org/10.1016/j.physd.2025.134896

25. Y. Jia, D. Wang, B. Shen, Z. Ju, Q. Huang, X. Wang, et al., Predicting ultrafast soliton evolution via a parameter-driven neural network, *Laser Photonics Rev.*, **20** (2026), e03212. https://doi.org/10.1002/lpor.202503212

26. R. Zhang, Z. Zhao, Y. Hu, J. Kang, Neural-symbolic exact solutions for Camassa–Holm equation, *Neurocomputing*, **706** (2026), 135040. https://doi.org/10.1016/j.neucom.2026.135040

27. Z. Zhao, R. Zhang, Artificial intelligence-enhanced mathematical derivation method: exact solutions of the Benjamin–Bona–Mahony equation, *Eng. Appl. Artif. Intell.*, **173** (2026), 114464. https://doi.org/10.1016/j.engappai.2026.114464

28. D. Wang, Z. Liu, H. Zhao, H. Qin, G. Bai, C. Chen, et al., Launching by cavitation, *Science*, **389** (2025), 935–939. https://doi.org/10.1126/science.adu8943

29. T. Chang, L. Hsiao, *The Riemann problem and interaction of waves in gas dynamics*, Harlow, Essex: Longman Scientific & Technical, 1989.

30. J. Smoller, *Shock waves and reaction–diffusion equations*, New York: Springer-Verlag, 1994. https://doi.org/10.1007/978-1-4612-0873-0

31. Q. Zhang, W. Sheng, Interaction of elementary waves for the Aw–Rascle traffic flow model with variable lane width, *Z. Angew. Math. Phys.*, **72** (2021), 175. https://doi.org/10.1007/s00033-021-01606-7

32. S. Fan, Y. Zhang, Riemann problem and wave interactions for an inhomogeneous Aw–Rascle traffic flow model with extended Chaplygin gas, *Int. J. Non-Linear Mech.*, **152** (2023), 104384. https://doi.org/10.1016/j.ijnonlinmec.2023.104384

33. E. Isaacson, B. Temple, Nonlinear resonance in systems of conservation laws, *SIAM J. Appl. Math.*, **52** (1992), 1260–1278. https://doi.org/10.1137/0152073



AIMS Press

© 2026 the Author(s), licensee AIMS Press. This is an open access article distributed under the terms of the Creative Commons Attribution License (https://creativecommons.org/licenses/by/4.0)